

Improved Swarm Engineering: Aligning Intuition and Analysis

John Harwell, *Member, IEEE*, and Maria Gini, *Fellow, IEEE*

Abstract—When designing swarm-robotic systems, systematic comparison of swarm control algorithms is necessary to determine which can scale up to handle the target problem size and operating conditions. Qualitative predictions of performance based on algorithm descriptions are often incorrect, and can lead to costly design processes for swarm-robotic systems. We propose a set of quantitative measures for swarm scalability, emergence, flexibility, and robustness which enable swarm control algorithms analysis and comparison, swarm performance of a given control algorithm, collectively enabling quicker and more confident design decisions. We demonstrate the utility of our proposed measurements as modeling and design tools for real-world scenarios by analyzing two common problems, indoor warehouse object transport and search and rescue, and present experimental results obtained in simulation.

Index Terms—Swarm Robotics, Swarm Engineering, Foraging.

I. INTRODUCTION

Swarm Robotics (SR) systems consist of large numbers of homogeneous groups of robots [1]. The main differentiating factors between SR systems and multi-agent robotics systems stem from the origins of SR as an offshoot of Swarm Intelligence (SI), which investigates algorithms and problem solving techniques inspired from natural systems such as bees, ants, and termites [2]. The main properties are:

- 1) *Scalability*. SR systems have no centralized control and no single point of failure, which makes them scalable to hundreds or thousands of agents, much like their natural counterparts [3]. We investigate swarm scalability by comparing how much work is done through agent cooperation vs. independent action (see Table I).
- 2) *Emergent Self-Organization*. Agents in SR systems collectively find solutions to a problem at hand that they cannot solve alone [4]. More precisely, emergent behaviors refer to the appearance of self-organization within the system due to robot interactions [5], [6]. Such behaviors cannot be predicted from individual agent behaviors (i.e., it is the set difference between micro and macro swarm behavior [7]). We investigate swarm emergent self-organization along two axes: (1) *spatial* self-organization, defined as collective optimization of inter-robot interference and movement patterns, and (2) *task-based* self-organization, defined as collective optimization of task allocation distributions (see Table I).

Work supported in part by Amazon Robotics, the MnDRIVE RSAM initiative at the University of Minnesota, and the Minnesota Supercomputing Institute

J. Harwell and M. Gini are with the Department of Computer Science and Engineering, University of Minnesota, Minneapolis, MN 55455, USA (e-mail: harwe006@umn.edu, gini@umn.edu)

Swarm Property	Property Measurement Axis 1	Property Measurement Axis 2
Scalability	Degree of Cooperation	N/A
Emergent Self-Organization	Spatial	Task-based
Flexibility	Reactivity	Adaptability
Robustness	Population Dynamics	Sensor and Actuator Noise

TABLE I: Taxonomy of the SR system properties and the axes along which we have derived quantitative measurements for each property.

- 3) *Flexibility*. In SR systems all decisions are made by individual agents based on locally available information from neighbors as well as their own limited sensor data. This results in reactive and adaptive swarm-level behaviors that attempt to mitigate adversity and exploit beneficial changes in dynamic environmental conditions and/or problem definitions which may be global or local [8], [9]. We investigate swarm flexibility along two opposing axes: (1) proportional *reactivity* to positive and negative temporal changes in the environment, (2) resistive *adaptivity* to positive and negative temporal changes in the environment (see Table I).
- 4) *Robustness*. Real robot sensors and actuators will always have errors even in the most tightly controlled environments; such errors may be very large in unstable or dangerous outdoor environments. In many conventional multi-agent systems such errors are handled analytically, if they are handled at all; SR systems typically rely on emergent behaviors to overcome such challenges. Furthermore, the number of agents in a SR system is unlikely to remain constant during execution; system size can fluctuate due to the introduction of new agents and existing agent failures. A high agent failure or task reallocation rate may slow swarm operation, but it does not prevent the accomplishment of the objective, in contrast to other multi-agent systems which cannot withstand such changes [3]. We investigate swarm robustness along two axes: (1) collective adaptation to temporally varying levels of *sensor and actuator noise*, and (2) collective adaptation to temporal changes in the swarm *population size* (see Table I).

Swarm engineering is an emerging sub-field in swarm robotics for the systematic application of scientific and technical knowledge to model, design, validate, and operate a swarm intelligence system [10], first formally discussed by [11]. Swarm engineering aims to provide mathematical tools to an-

swer the following crucial design questions when considering a set of potential solution systems for a given application suitable for SR derived solutions:

- 1) Which solution can scale best to the current and future needs of the modeled scenario?
- 2) Which solution shows the highest level of emergent self-organization, indicative of its potential to be used in variants of a given problem, helping to “future-proof” design decisions?
- 3) Which solution is the most reactive and adaptable to *external* fluctuations in environmental conditions, suggesting its relative ease in crossing the simulation-reality gap [12]?
- 4) Which swarm control algorithm is the most robust to *internal* fluctuations in swarm state (sensor/actuator noise, population size)?

The contributions of this paper are to the sub-field of swarm engineering as follows:

- 1) Formal presentation of measurement methods for each of the core SR principles: scalability (Section IV-A), emergence (Section IV-B), flexibility (Section IV-C), and robustness (Section IV-D), to augment the set of mathematical tools available to SR system designers. Our methodology enables greater insight into and predictive power over swarm response to external and internal stimuli, which would be difficult or impossible to do by simply looking at raw performance measurements.
- 2) Advancement of the state of the art in modeling characteristics of real-world problems made possible by our measurement methods (Section III-A).
- 3) Demonstration of the utility of our methodology in comprehensively answering the SR system design questions posed above through their application to two real-world foraging problems: indoor warehouse object transport (Section VI) and outdoor search and rescue in unknown environments (Section VII). Furthermore, our methodology is shown to support our intuition in answering the SR system design questions on each scenario, making a strong case for its inclusion in any swarm engineer’s toolbox.

A preliminary version of this paper was published in IJCAI 2019 [13]. That paper provided quantitative measurements of scalability, emergent self-organization, and flexibility, and evaluated them in an indoor warehouse setting. This paper extends our previous work in the following ways:

- We have refined our previous measures on scalability, emergent self-organization, and flexibility to be more intuitive and grounded in the current state-of-the-art.
- We have defined a quantitative measure for the fourth SR system property: robustness.
- In addition to evaluating our four measures in an indoor warehouse setting, we also evaluated them in a scenario with substantially different characteristics: outdoor search and rescue.
- The set of swarm control algorithms used for comparison in each scenario has been expanded from three to

four, and a much more comprehensive analysis has been performed.

The rest of the paper is organized as follows. In Section II we discuss related work in terms of their contribution to advancing the understanding of the swarm properties of scalability, emergent self-organization, flexibility, and robustness. In Section III, we discuss two motivating real-world problems and we compare swarm control algorithm and their associated design constraints in the context of swarm engineering: object transport in an indoor warehouse and civilian search-and-rescue in a disaster zone. In Section IV, we present our proposed quantitative measurements for the swarm properties, providing theoretical derivations for each. In Section VI and Section VII we apply our proposed measures to the indoor warehouse object transport and search-and-rescue problems, respectively, and discuss results. We conclude with a brief discussion in Section VIII, and present conclusions and some directions for future work in Section IX.

II. BACKGROUND AND RELATED WORK

Previous work directly focused on swarm engineering has focused on theoretically derived algorithm design and/or provability of system properties [11]. In general, most recent work in theoretical ([14]–[19]) or heuristic ([20]–[22]) control algorithms for swarms focuses on the presentation of the algorithm, and possibly with proving properties. However, very few works consider *how* to quantify the behavior of the swarm in real world settings; one such work is [13]. Consider which of the following systems would have greater real-world utility: a heuristic control algorithm with no provable guarantees but good performance on many problems of interest, or a rigorously derived control algorithm with many theoretical guarantees but relatively poor performance on real-world problems of interest? Depending on the application parameters, stakeholders, and many other factors, either algorithm may be considered the “best”.

Generally speaking, the “best” algorithm is created iteratively through qualitative means: testing, algorithmic study, etc. The number of iterations can be reduced in two ways. First, through more accurate problem modeling. Second, through quantitative measurements of principles in such a way that performance on variants of a given evaluated problem can be accurately predicted for a given iteration. However, to the best of our knowledge, a design methodology encompassing both of these does not exist, and is a major reason why there has not been more extensive application of swarm intelligence to real-world problems [23]. Previous work ([8], [13], [24]) in swarm engineering directly investigating algorithms for a target application only implicitly considers the swarm properties of scalability, emergent self-organization, robustness, and flexibility through raw performance comparisons (with the exception of [13], which presented a methodology partially capable of (1) and (2)).

Sahin ([1]) defines the lower bound for the number of agents that must be present in order for a system to be considered a swarm to be between 10–20. However, many recent works such as [19], [25], [26], do not even meet this standard.

In recent years, many theoretical SR system design tools have become available [19], [27]–[29]. These tools have made it easier to conduct mathematical analysis of algorithms and derive analytical, rather than weakly inductive proofs of correctness [9]. Despite this, there has not been a corresponding increase in the average swarm sizes used to evaluate new algorithms for tackling problems of real-world scale (notable exceptions include [28] (600 robots), [12] (768 robots), [30] (375 robots), [13] (16,384)). Investigation of simple behaviors such as pattern formation, localization, or collective motion, where design and computational complexity do not inherently limit scalability, is generally evaluated with relatively small scales ([31] (20 robots), [9] (40 robots)). Methods for more complex behaviors are likewise tested at similar scales: foraging [22], [32] (20 robots), [26] (30 robots), task allocation [19] (25 robots). While such sizes technically meet Sahin’s criteria, they fall short of their biological origins (i.e. thousands, if not millions, of agents). From a swarm engineering perspective, they may not provide enough confidence in algorithm correctness, since emergent behaviors arise only at larger scales. Furthermore, studies at small scales may suffer from unmanifested theoretical and empirical scalability issues.

We believe that the lack of evaluation of large SR systems is partially due to a lack of insightful, predictive measurement methods to accurately characterize swarm performance across problem scales and domains. Building on previous works [8], [12], [33], we propose a swarm scalability measure analogous to speedup when core count is increased on supercomputing clusters in Section IV-A.

Within SR, no widely accepted theory of self-organizing systems exists [6], [30]. However, some common properties of self-organizing swarm systems have been observed and/or proposed [34]. Let \mathcal{S} be a swarm of size \mathcal{N} robots, then the properties are:

- 1) *Positive feedback*. Simple behavioral heuristics which promote the creation of convenient structures at the collective level, such as reactive recruitment and reinforcement via trail laying and following in some ant species or dances in bees. Positive feedback in the presence of constrained physical environments can lead to emergent spatial self-organization [35].
- 2) *Negative feedback*. Counterbalances positive feedback and helps stabilize the collective behavior of \mathcal{S} . In natural systems, negative feedback mechanisms, such as pheromone evaporation, have evolved to avoid potential saturation in terms of available foragers, food source exhaustion, crowding or competition at the food sources, etc, as studied in [8], [36].
- 3) *Random fluctuations*. Random walks, sensor/actuator errors, random task switching among swarm individuals are necessary for collective creativity, innovation, and problem solving, though they can also lead to sub-optimal collective solutions if not moderated by the other self-organizing properties.
- 4) *Multiple interactions*. Robots in \mathcal{S} use the information coming from the other robots (possibly through joint environment manipulation) to choose how to act, and more interactions can lead to more informed decisions.

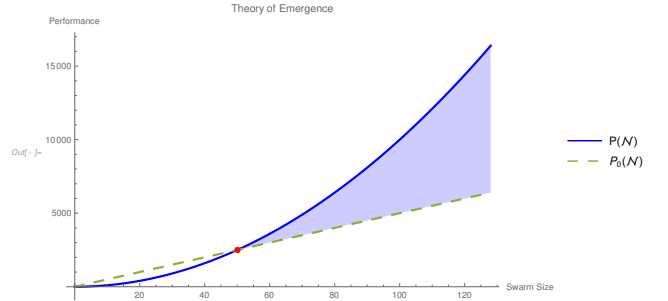


Fig. 1: Example of emergent swarm intelligence: $P(\mathcal{N}) - P_0(\mathcal{N})$, where $P_0(\mathcal{N})$ is the performance attained by \mathcal{N} independent robots, and $P(\mathcal{N})$ is the performance achieved by \mathcal{N} interacting robots. Emergence swarm intelligence is achieved when $\mathcal{N} \geq 50$ in this instance (shaded region).

A control-theoretic model of emergence presented in [4] distinguished between *complicated* systems which can be studied by the methods of scientific reductionism, and *complex* systems which originate from the existence of a threshold above which interaction between system components overtakes outside interactions, leading to system self-organization and new behavior not predictable from component study, similar to [37]. Furthermore, emergent system properties can only be observed (1) after a sufficiently long observation window has elapsed, and will be absent when observed in a single snapshot or short time intervals, and (2) in the global view of the system, and will be absent when observed in the local view of single agent or a small group of agents [38]. While many papers cite evidence that their algorithms exhibit emergent behavior ([8], [27], [39], [40]), or provide a framework for logical reasoning about emergent properties ([5], [38]), few study emergent behavior quantitatively; exceptions include [7], [8], [41], [42].

An early analysis of emergent behavior presented by [43], posited that a swarm composed of \mathcal{N} units only exhibits emergent behavior when \mathcal{N} exceeds a critical size \mathcal{N}_c . Below this threshold, swarm attempts at self organization can negatively affect performance (Fig. 1, unshaded region). A more generalized definition defined emergence as the *positive difference* $P(\mathcal{N}) - P_0(\mathcal{N})$ [41], [42] (Fig. 1, shaded region). $P(\mathcal{N})$ is the amount of performance achieved by a swarm of \mathcal{N} interacting robots, and $P_0(\mathcal{N})$ is the amount of performance achieved by an equivalent swarm of independent agents.

We extend and formalize this intuition (also mentioned by [23]) in Section IV-B along two axes as a step towards the development of a more general emergence theory. First, we present a method for measuring the level of spatial self organization present in a swarm by measuring the sub-linearity of inter-robot interference as swarm size \mathcal{N} increases. Second, we present a method for measuring the level of task-based self-organization in a swarm by measuring the super-linearity of marginal performance gain as swarm size increases [44].

Flexibility among agents within a swarm in response to internal and external changes is an important aspect of their collective utility. Swarms should be able to *react* to quality factors in the environment, such as the quality or safety

of locations within the arena, while also *not* changing their behavior in response to every fluctuation in the external environment (*resistivity*). Many works on flexibility compare the performance of swarm control algorithms under environmental conditions different than their development [12], [21], [25]. However, the resultant claims of flexibility due to performance similarity across scenarios is strictly qualitative, due to a lack of mathematical quantification of “difference” in scenario conditions as a factor in performance comparisons. Building on the mathematical curve similarity methods from Jekel *et al.* [45], who tested different mathematical curve similarity measures in various noise and normalization conditions, and the above intuition, we derive a temporally-aware measure quantifying the difference between expected and observed performance in arbitrary environmental conditions, and use it to quantify swarm *reactivity* and *adaptability* in Section IV-C.

Swarm robustness to agent losses was studied by [46] from a control-theoretic perspective using filtering for a distributed search and rescue task. Availability analysis, i.e., determining what fraction of a swarm will be available on average in statistical equilibrium to work on tasks, given robot malfunction and repair rates, by [47] investigated both independent and coupled robot malfunction rates. Queueing-theoretic methods reduced the requirement for the number of taxis needed to meet demand in a large city [48].

In queueing theory, queues are described by a tuple $A/S/c/K/N/D$ [49]. A is the arrival process, which is typically Markovian; S is the service time distribution, which is also typically Markovian; c is the number of service channels available to service items as they leave the queue; K is the number of places in the queue; N is the size of the calling population from which items enter the queue; and D is the queue’s “discipline” (FIFO, LIFO, random, etc.). In general, most queues can be described by $A/S/c$, where the omitted values are assumed to be $\infty/\infty/FIFO$. The most commonly studied queue is the $M/M/1$ queue, in which items arrive at rate $\sim Poisson(\lambda)$, remain in the queue for a period of time, and are serviced at rate $\sim Exp(\mu)$ [49]. Under these assumptions, it is possible to describe the behavior of the system using Markov models. Using this mathematical basis and the work of [47], we derive expressions for the average number of robots in the system and how long a robot stays in the system, and use this to define a population dynamics robustness measure in Section IV-D.

Recent works in swarm robustness have considered robustness as collective resistance to sensor and actuator noise. The effect of Gaussian noise distributions on collective swarm motion was measured and empirically analyzed by [18], [31]. It was shown that swarms in general are able to adapt and overcome Gaussian distributed noise with $\sigma = \pm \frac{\pi}{2}$ in many cases, but for $\sigma = \pm\pi$ or greater, only small swarms are able to adapt [18]. Gaussian noise distributions were applied to robot sensor readings in [24], and their effects studied for different variants of adaptive response threshold foraging algorithm. The Fokker-Planck equation was derived from statistical physics for a given Langevin equation governing robot motion, including noise models, and applied to the analysis of simple phototaxis behaviors [30]. Other works

inject a small level of uniform or Gaussian noise (0.5–10%) to help narrow the simulation-reality gap, without performing statistical analysis ([12], [32]). Many theoretic works do not incorporate noise into their models ([15], [17], [50], [51]); exceptions include [18]. Similarly, many application oriented works do not systematically evaluate algorithms in the presence of noise ([8], [13], [39]); exceptions include [24].

Using the mathematical curve similarity measures from [45] as a basis, we derive a temporally-aware measure for quantifying the difference between expected and observed performance in arbitrary environmental conditions, and use it to quantify swarm robustness to sensor and actuator noise in Section IV-D.

III. APPLICATION SCENARIOS OVERVIEW

The duality between SR and natural systems enables effective parallels to be drawn with many naturally occurring problems, such as foraging, collective transport of heavy objects, environmental monitoring, hazardous material cleanup, self-assembly, exploration, and collective decision making [1], [2], [12], [52]. As a result, SR systems are especially well suited to tackle complex tasks in environments where robustness and flexibility are keys to success, such as space [53].

We examine two common application scenarios: indoor warehouse object transport (Section VI), and outdoor search and rescue (Section VII), framed as swarm control algorithm selection problems. These applications span different problem domains in which SR systems have been successfully applied, and thus serve as excellent testbeds for determining the utility of our proposed methodology as an assistive tool in the development of SR systems.

We study our two scenarios as *foraging tasks*. In a foraging task, robots gather objects from across a finite operating arena and bring them to a central location under various conditions and constraints. Foraging is studied extensively in SR, due to its straightforward mapping to real-world applications.

A. Design Constraints

We begin by describing common design constraints which may be present in each of our application scenarios *before* the subsequent derivation of our measurement methods for scalability, emergence, robustness, and flexibility (Section IV), helping to ensure their utility beyond the scope of this work.

Efficiency. For most applications, viable SR solutions will need to maintain efficiency as the problem scales; that is, adding more robots to tackle a larger problem instance will result in proportionally greater performance. If exponential performance drop off were acceptable as swarm and/or problem size is increased, then many non-swarm, centralized approaches to robot coordination could be employed instead (probably to greater effect than swarm-based approaches).

Environmental Disturbances. In many instances, it may not be feasible to develop and test SR systems in the exact environmental conditions in which they will operate (e.g., space, military, disaster cleanup applications) due to cost or locality constraints [54], [55]. Therefore, flexibility in reacting and adapting to potentially unknown conditions is critical.

Noisy environments. In many environments, sensor and actuator readings may not be accurate (beyond the usual level of noise). Levels of noise can vary (1) depending on the robot’s current location within the operating arena, and (2) the current time (e.g., temporally varying sources). In this work, we consider a noise model in which the exact noise level is not known *a priori*, but its distribution is known or can be reasonably inferred. We further assume that whatever the current level of sensor and actuator noise present at a robot’s current location at time t , it effects all sensors and actuators equally; this assumption may be relaxed in the future.

Unreliable robots. All robots are fallible, due to the nature of robotic hardware (and possibly latent software bugs); it is only a question of how often they fail and if the failure is permanent or repairable. Prior work on the effect of robotic failures [47] only considers temporary failures, and does not consider their effect on cumulative performance; we expand the scope of that work by considering the effect of temporary and permanent robot failures.

Semi-adversarial task reallocation. Given the inherent flexibility to adapt and learn to perform different tasks efficiently, it is reasonable that not all robots within a swarm will be working on the same task at the same time, as different system operators dynamically reallocate swarms and sub-swarms to tasks in real-time. Previous work in swarm robotics in general, and foraging in particular, assumed that system operators will have exclusive use of the entire swarm (of whatever size) for the task at hand (i.e., $\mathcal{N} = N(t)$ for all t) ([8], [12], [13], [32], [56]). For simplicity of analysis, we assume that all robot reallocations are independent and can happen at any time; future work may explore more complex reallocation models.

Operating arena size. If the size of the area in which S will operate in is known beforehand, *variable swarm density* is an appropriate model, in which swarms of increasing size \mathcal{N} are placed in the same spatial area and their behavior measured. If the size of the area in which S will operate in is not known beforehand, *constant swarm density* is a more appropriate model, in which the size of the operating area scales linearly with increasing \mathcal{N} . Our definition of swarm density here loosely falls under the Eulerian continuum for swarm dynamics, as described in [57].

The choice of variable or constant swarm density as part of modeling requirements is a critical factor in the design process. As swarm sizes are increased with variable density, robots in swarms with higher densities will experience *more* inter-robot interactions than robots in smaller swarms, thus skewing the results of the measurements defined in Section IV. As swarm sizes are increased with constant density, arena size also increases proportionally, greatly reducing skewing artifacts. An appropriate model needs to be chosen in either case, as swarm density, not size, is the critical factor in determining swarm emergent self-organization [42].

Object Distribution. The distribution of objects to be gathered in the operating arena can be modeled in various ways. The most common distribution is *random* (Fig. 2d), in which objects are scattered uniformly in a square or circular environment [12], [17], [24], [42]. The *single source* distribution (Fig. 2a) has also been extensively studied [8], [13], [22], [26],

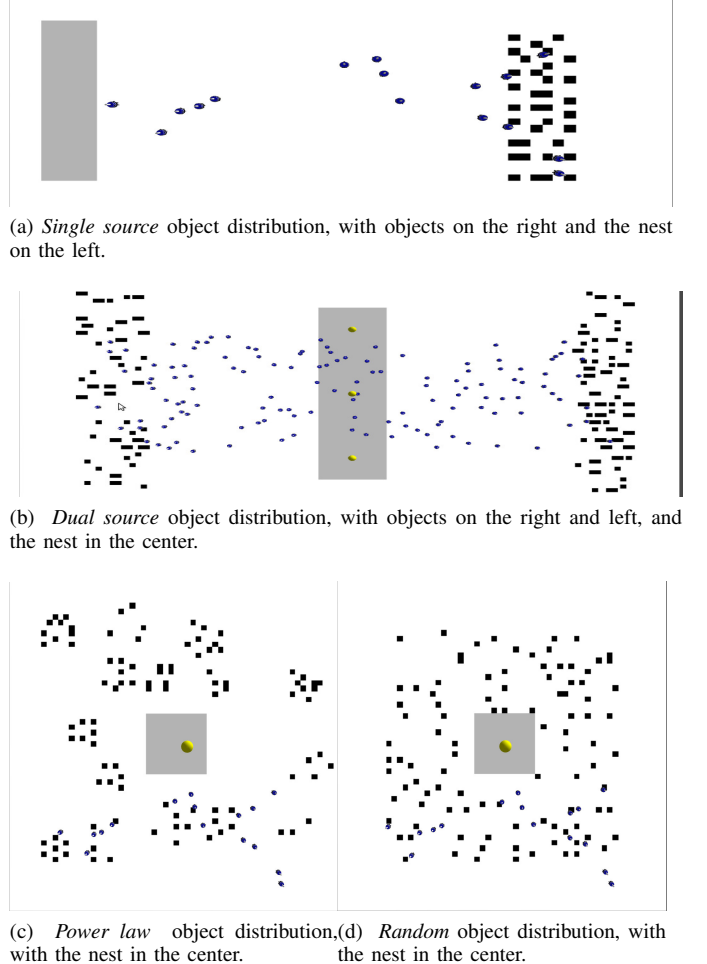


Fig. 2: Example foraging distributions.

[32], [56]. Other studied distributions include *dual source* [56] (Fig. 2b), in which objects are concentrated on either side of the collection site in a rectangular arena, and *power law* (Fig. 2c), in which objects are clustered in groups of various sizes [12]. When the object distribution is not known or cannot be inferred a priori, *random* or *power law* are appropriate, following empirical observations [12].

Minimum collective performance. In SR applications with task reallocation and/or robotic failures (temporary or permanent), a common design constraint is a minimum performance that $S \in \mathcal{S}$ must meet in statistical equilibrium as $N(t)$ fluctuates. We utilize the notion of *swarm availability*, and define p_v as the probability that N_{min} robots from a swarm of size \mathcal{N} are allocated to task \mathcal{T} at t (for a derivation, see [47]):

$$\begin{aligned}
 p_v &= \pi_{\mathcal{N}} \left(1 + \sum_{k=N_{min}}^{\mathcal{N}-1} \prod_{i=k+1}^{\mathcal{N}} \frac{\mu_S}{\lambda_S} \right) \\
 &= \pi_{\mathcal{N}} \left(1 + \sum_{k=N_{min}}^{\mathcal{N}-1} \prod_{i=k+1}^{\mathcal{N}} \frac{1}{\rho} \right)
 \end{aligned} \tag{1}$$

Using Eq. (1) we can now solve for either:

- ρ , obtaining a *ratio* that the rates of robots entering/leaving S must satisfy if (p_v, N_{min}) are specified as part of the SR design process.

- A range of achievable p_v given the rates of robots entering/leaving \mathcal{S} , and a range of N_{min} values. Fig. 11a shows an example of these curves of achievable availability, computing steady state swarm sizes from Eq. (11), plotted against a range of N_{min} .

B. Candidate Algorithms Overview

We have selected several state-of-the-art foraging swarm control algorithms (κ), summarized briefly here, for analysis in our two scenarios [8], [56]. We include intuitions about how each controller will perform in terms of scalability, self-organization, flexibility, and robustness, based solely on their technical descriptions, so that we can determine to what extent our intuitions are embodied by the results of our two scenarios.

- In *Correlated Random Walk (CRW)* swarms, robots perform a correlated random walk until they acquire an object, which they then transport to the nest using phototaxis (i.e., motion in response to light). Robots do not perform task allocation.

We do not expect high levels of self-organization in CRW swarms, because they perform random walks and are purely reactive; we expect relatively high levels of sensor and actuator robustness for the same reason. We expect high levels of reactivity because robots only have a single mode of operation, regardless of environmental conditions, and will be substantially affected by changes in adversity.

- In *Decaying Pheromone Object (DPO)* swarms, robots track seen objects using exponentially decaying pheromones, and determine the “best” object to acquire using derived information relevance. Robots do not perform task allocation.

In spatially constrained and unconstrained environments we expect lower levels of self-organization and scalability than CRW swarms in constrained spaces; the competition at shared resources (e.g., foraging targets) due to robot memory will likely outweigh its benefits, especially as time goes on and the swarm collectively learns where clusters of objects of interest can be found. In unconstrained spaces, we expect higher levels of self-organization and scalability.

- In *STOCHM* swarms, robots stochastically choose to do either (1) the entire foraging task themselves (i.e., retrieving an object and bringing it to the nest), or (2) one of two subtasks of bringing an acquired object to a *static* intermediate drop site (cache), or picking one up from a cache and bringing it to the nest. These three tasks form a *compound* task decomposition graph (Fig. 3, gold tasks [56]), in which an overall task can be decomposed into smaller, simpler tasks exactly one way.

STOCHM swarms will also suffer from congestion near the locations of static caches, which may outweigh the self-organization possible due to multiple tasks. We also expect higher levels of scalability and reactivity than DPO swarms in constrained spaces, due to (1) the presence of caches to help regulate traffic, and (2) the maintenance of the caches by an outside process independent of swarm

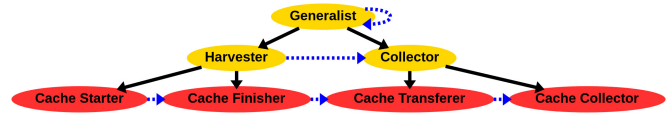


Fig. 3: Task decomposition graph. Solid edges indicate task decomposition, dashed blue edges indicate dependent task sequences. Gold tasks define *compound* task decomposition, red+gold tasks define *complex* task decomposition.

behavior. In unconstrained spaces, we expect lower levels of scalability and reactivity. The sensor and actuator robustness of STOCHM swarms should be very similar to DPO swarms, but the population dynamics robustness should be higher, because some of the information about the world model carried by robots is now encoded in the environment, and the ability to choose from multiple tasks should also improve collective re-convergence to an efficient steady-state.

- In *STOCHX* swarms, robots can stochastically choose any of the tasks of the STOCHM algorithm (i.e. exploit existing caches) to perform, but can also choose to perform tasks related to dynamically creating new caches as simulation conditions evolve. Robots perform task allocation, according to the STOCH-N1 algorithm [56], a stochastic choice depending on the location of the most recently executed task within the graph of tasks available to each robot. The available tasks form a *complex* task decomposition graph (Fig. 3, red+gold tasks), in which an overall task can be decomposed into smaller, simpler tasks in multiple ways.

The dynamic creation of caches should eliminate the negative effects of congestion near caches we expect with STOCHM, and result in high levels of self-organization; we expect greater flexibility and population dynamics for the same reason. However, raw performance may be lower than other algorithms because the swarm has to perform additional cognitive work throughout operation regarding dynamic cache management (e.g., exploration vs. exploitation of the environment).

IV. PROPOSED QUANTITATIVE MEASUREMENTS

In this section we derive quantitative measurement methods for swarm scalability (Section IV-A), emergent self-organization (Section IV-B), flexibility (Section IV-C), and robustness (Section IV-D). Our formulations of these measurements are motivated by the common SR design constraints presented in Section III-A, and are designed to have utility beyond the scope of this work.

- We measure swarm scalability in terms of the cooperative vs. independent portions of swarm performance.
- We measure swarm emergent self-organization across population sizes in terms of expected vs. actual performance losses (*spatial* self-organization), and expected vs. actual performance gains (*task-based* self-organization).
- We measure swarm flexibility by correlating temporal curves of swarm performance with curves of varying

environmental conditions, quantifying swarm *reactivity* (how closely swarm performance tracks changing environmental conditions in time) and *adaptability* (how well the swarm exploits or resists beneficial or adverse changes in environmental conditions).

- We measure swarm *robustness* in terms of (1) its collective resilience to robot sensor and actuator noise (*Sensor and Actuator* robustness) again using mathematical methods of curve similarity, and (2) its collective resilience to temporally changing swarm sizes (*Population Dynamics* robustness) extending the queueing-theoretic model developed by [47] to encompass robot failures (temporary and permanent), and robot reallocations to non-foraging tasks (temporary and permanent).

In the subsections below, let \mathcal{S} be a swarm composed of \mathcal{N} homogeneous robots. Let κ be the swarm control algorithm plus algorithmic parameters present on each robot in \mathcal{S} , and t the current discrete timestep. We can then define $P(\mathcal{N}, \kappa, t)$, an arbitrary performance measurement of some aspect of the behavior of \mathcal{S} : time to complete a certain number of tasks, task completion rate, etc. $P(\mathcal{N}, \kappa, t)$ will vary across κ , and will trace out a temporally varying performance curve, measurable at every t . This formulation of swarm performance allows us to simultaneously analyze (1) cumulative performance by summing across all $t \in T$ (see Sections IV-A and IV-B), and (2) temporally varying performance curves via pairwise point comparison for each $t \in T$ (see Section IV-C, Section IV-D).

We place the following restrictions on $P(\mathcal{N}, \kappa, t)$:

- 1) $P(\mathcal{N}, \kappa, t) \geq 0$ for all t .
- 2) If κ_1 is considered to be better than κ_2 at time t , then $P(\mathcal{N}, \kappa_1, t) > P(\mathcal{N}, \kappa_2, t)$. This is not a restrictive assumption, as performance measures where smaller values are better (e.g., average time to task completion), can be made to satisfy this assumption by taking their reciprocal at each t .

Let $I_{ec}(t)$ and $V_{dev}(t)$ be continuous, one-dimensional signals, where $I_{ec}(t)$ represents the ideal environmental conditions that a given swarm was developed in, and $V_{dev}(t)$ is the signed waveform of an adverse deviation from $I_{ec}(t)$, where positive values indicate increased adversity in environmental conditions when compared with $I_{ec}(t)$, and negative values indicate decreased adversity in environmental conditions.

$P_{ideal}(\mathcal{N}, \kappa, t)$ and $P(\mathcal{N}, \kappa, t)$ are one-dimensional signals, where $P_{ideal}(\mathcal{N}, \kappa, t)$ represents the performance of a given algorithm κ controlling \mathcal{S} under ideal conditions, and $P(\mathcal{N}, \kappa, t)$ represents the performance of a given algorithm κ controlling \mathcal{S} under non-ideal conditions. We have restricted our study to one-dimensional characterizations of environmental conditions in this work, but extensions to higher dimensions should be relatively straightforward.

A. Swarm Scalability

Previous work calculated swarm scalability as $S(\mathcal{N}) = P(\mathcal{N})/\mathcal{N}$ (i.e., per-robot efficiency) [12]. While this measure provides insight into scalability, it is not predictive (e.g. given $P(\mathcal{N})$, we cannot plausibly estimate $P(2\mathcal{N})$ without retroactively charting $S(\mathcal{N})$ across a range of values for \mathcal{N}).

We apply the more general $P(\mathcal{N}, \kappa, t)$ measurement to define a more predictive scalability measure for use as an iterative system design tool by adapting the Karp-Flatt metric [33]. Traditionally, the *serial fraction* e of the Karp-Flatt metric measures the level of parallelization of a particular program, with smaller values indicating high parallelization and plausibly expected speedups if more computational resources are added. We have adapted it to measure the scalability of a swarm by exposing the part of $P(\mathcal{N}, \kappa, t)$ that did not utilize inter-robot cooperation, with smaller values indicating high levels of cooperation and plausible efficiency increases if \mathcal{N} is increased, thereby creating a *predictive* scalability measure.

Intuition: Robots within a swarm of size \mathcal{N} are analogous to processors or nodes in a High Performance Computing (HPC) system: if a job takes T seconds with \mathcal{N} resources, ideally it will take $T/2$ seconds with $2\mathcal{N}$ resources in a perfectly parallelizable system.

Definition: $\mathcal{C}(\mathcal{N}_1, \mathcal{N}_2, \kappa)$, where $\mathcal{N}_1 < \mathcal{N}_2$, is defined as:

$$\mathcal{C}(\mathcal{N}_1, \mathcal{N}_2, \kappa) = \sum_{t \in T} 1 - \frac{P(\mathcal{N}_2, \kappa, t) - \frac{1}{\mathcal{N}_2/\mathcal{N}_1}}{1 - \frac{1}{\mathcal{N}_2/\mathcal{N}_1}} \quad (2)$$

The right-hand side of the minus in Eq. (2) is the serial fraction e of the Karp-Flatt metric, where we have defined “speedup” as the performance gain with \mathcal{N}_2 robots over the performance with \mathcal{N}_1 robots, rather than over the performance with 1 robot, per the original paper. This is because some κ perform very poorly with small numbers of robots (i.e., substantially sub-linear increases in performance across relatively small \mathcal{N}), while some κ have more linear increases in performance across relatively small \mathcal{N} .

We note that negative values for $\mathcal{C}(\mathcal{N}_1, \mathcal{N}_2, \kappa)$ are possible, due to the fact that the original Karp-Flatt metric we used as a basis assumes that performance is a monotonically increasing function (i.e., adding more processors always gives some marginal gain), and this assumption is not valid in general for SR systems when adding more robots.

B. Swarm Emergent Self-Organization

We can infer from Cotsaftis [4] that SR systems with a high degree of local interactivity should exhibit higher levels of self-organization (and therefore emergent behavior [37]) than systems with a low degree of interactivity [5]–[7].

From Fig. 1, we know that emergent behavior can be quantitatively measured as a super-linear increase in swarm performance as \mathcal{N} increases linearly. We argue sub-linear increases in the observed level of inter-robot interference across linearly increasing \mathcal{N} are *also* indicative of emergent behavior. We therefore define a swarm’s emergent behavior along two axes. First, *spatial* self-organization, defined as collective optimization of inter-robot interference and movement patterns. Second *task-based* self-organization, defined as collective optimization of task allocation.

In order for spatial self-organization to emerge \mathcal{S} must be operating in a bounded space; without this restriction a swarm will not necessarily be collectively motivated to manage space efficiently. In applications such as outdoor search and rescue,

with large or unbounded operating arenas, a task-based self-organization measure may be more appropriate. For other applications, assuming a bounded space is reasonable. For example, such restrictions are common in real-world indoor applications such as warehouses [26], [46].

1) Spatial Emergent Self-Organization:

Intuition: If the proportional increase in the amount of performance *lost* due to inter-robot interference between swarms of size \mathcal{N}_1 and \mathcal{N}_2 ($\mathcal{N}_2 > \mathcal{N}_1$) is sub-linear, then self organizing has occurred. In the absence of self-organizing, random robot motions would produce \sim linear increases in the level of inter-robot interference as $\mathcal{N}_1 \rightarrow \mathcal{N}_2$ linearly. That is, the swarm has learned to leverage inter-robot interactions to become *more* spatially efficient with increasing \mathcal{N} .

Derivation: We calculate (post-hoc) the number of robots experiencing inter-robot interference (as opposed to doing useful work) within \mathcal{S} on each timestep t , denoted as $t_{lost}^{\mathcal{N}}(t)$. This can then be used to compute the per-timestep fraction of overall performance loss $P_{lost}(\mathcal{N}, \kappa, t)$ as follows:

$$P_{lost}(\mathcal{N}, \kappa, t) = \begin{cases} P(1, \kappa, t)t_{lost}^1(t) & \text{if } \mathcal{N}=1 \\ P(\mathcal{N}, \kappa, t)t_{lost}^{\mathcal{N}}(t) & \\ -\mathcal{N}P_{lost}(1, \kappa, t) & \text{if } \mathcal{N}>1 \end{cases} \quad (3)$$

For $\mathcal{N} > 1$ we subtracted the interference that would have occurred in a non-interactive swarm of \mathcal{N} robots (i.e. a swarm of size \mathcal{N} in which robots never interfered with each other). If we compute Eq. (3) for two swarms of size \mathcal{N}_1 and \mathcal{N}_2 with $\mathcal{N}_2 > \mathcal{N}_1$, then sub-linear increases that κ is scalable in the neighborhood of \mathcal{N}_2 . That is, doubling the swarm size does not double the amount of inter-robot interference. Eq. (3) quantifies a swarm's ability to detect and eliminate non-cooperative situations between agents [37] (e.g., frequent inter-robot interference) as \mathcal{N} is increased.

Definition: $E_S(\mathcal{N}_1, \mathcal{N}_2, \kappa)$ for two swarms of sizes \mathcal{N}_1 and \mathcal{N}_2 , with $\mathcal{N}_2 > \mathcal{N}_1$, is defined as:

$$E_S(\mathcal{N}_1, \mathcal{N}_2, \kappa) = \sum_{t \in T} \frac{\mathcal{N}_2}{\mathcal{N}_1} P_{lost}(\mathcal{N}_1, \kappa, t) - P_{lost}(\mathcal{N}_2, \kappa, t) \quad (4)$$

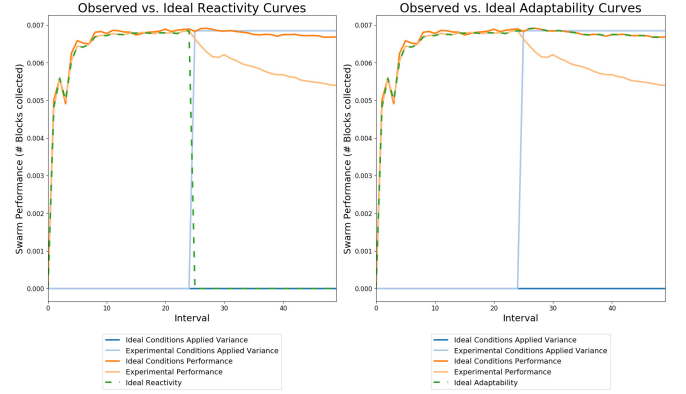
2) Task Emergent Self-Organization:

Intuition: Similar to our spatial self-organization axis, if a super-linear increase in the amount of performance *gained* due to optimization of higher level swarm functions is observed between two swarms of size \mathcal{N}_1 and \mathcal{N}_2 ($\mathcal{N}_2 > \mathcal{N}_1$), then self-organizing has also occurred. That is, the swarm has collectively learned to leverage inter-robot interactions and/or relationships between tasks to become *more* efficient with increasing \mathcal{N} .

Definition: $E_T(\mathcal{N}_1, \mathcal{N}_2, \kappa)$ for two swarms of sizes \mathcal{N}_1 and \mathcal{N}_2 , with $\mathcal{N}_2 > \mathcal{N}_1$ is defined as:

$$E_T(\mathcal{N}_1, \mathcal{N}_2, \kappa) = \sum_{t \in T} P(\mathcal{N}_2, \kappa, t) - \frac{\mathcal{N}_2}{\mathcal{N}_1} P(\mathcal{N}_1, \kappa, t) \quad (5)$$

It quantifies the *marginal performance gain* [44] of the swarm as superlinear increases in self-organization through performance.



(a) Example ideal reactivity $P_{R^*}(\mathcal{N}, \kappa, t)$. (b) Example ideal adaptability $P_{A^*}(\mathcal{N}, \kappa, t)$.

Fig. 4: Example ideal reactivity and adaptability $I_{ec}(t) = 0$ for all t , with $V_{dev}(t)$ is a step function.

C. Swarm Flexibility

We define a swarm's *flexibility* along two axes: its ability to quickly (1) *react* to changes in the external environment over time, and (2) *adapt* to changes in the external environment over time. These changes can include the cost of performing a particular action (e.g., picking up/dropping an object in the case of foraging), maximum robot speed (e.g., wheeled robots buffeted in variable winds in outdoor environments) or the performance of some tasks more slowly than others (e.g., carrying objects of greatly differing weights).

1) Reactivity:

Intuition: Swarm *reactivity* measures how closely the observed performance curve $P(\mathcal{N}, \kappa, t)$ tracks an applied variance $V_{dev}(t)$ when compared across all $t \in T$. That is, as environmental conditions improve or worsen over time, performance proportionally improves or worsens over time as well, as shown in Fig. 4a.

Derivation: We derive the performance curve of a swarm with optimal reactivity, $P_{R^*}(\mathcal{N}, \kappa, t)$, by noting that an optimally reactive swarm will react *instantaneously* and *proportionally* whenever $V_{dev}(t)$ is non-zero. Define c_t as a per-timestep constant representing the signed proportional difference between ideal and non-ideal conditions:

$$c_t = \frac{V_{dev}(t) + I_{ec}(t)}{I_{ec}(t)} \quad (6)$$

Then, $P_{R^*}(\mathcal{N}, \kappa, t) = c_t P_{ideal}(\mathcal{N}, \kappa, t)$ for all $t \in T$.

Definition: $R(\mathcal{N}, \kappa)$ is defined as:

$$R(\mathcal{N}, \kappa) = DTW(P_{R^*}(\mathcal{N}, \kappa, t), P(\mathcal{N}, \kappa, t)) \quad (7)$$

where we define $DTW(X, Y)$ to be a *Dynamic Time Warp* similarity measure between two discrete curves X and Y , based upon the conclusions in [45]. We note that (1) DTW correctly matches temporally shifted sequences of applied variance and observed performance (achieving $R^*(\mathcal{N}, \kappa)$ is not possible for realistic swarms), (2) DTW exhibits robustness to signal noise, and SR systems are inherently stochastic.

2) Adaptability:

Intuition: Swarm *adaptability* measures the swarm ability to (1) minimize performance losses under adverse conditions ($V_{ec}(t) > 0$), and (2) resist performance increases under beneficial deviations from ideal conditions ($V_{ec}(t) < 0$). That is, if non-ideal environmental conditions get better (or worse) over time, performance does *not* change from that in ideal environmental conditions, as shown in Fig. 4b.

Definition: $A(\mathcal{N}, \kappa)$ is defined as:

$$A(\mathcal{N}, \kappa) = DTW(P_{ideal}(\mathcal{N}, \kappa, t), P(\mathcal{N}, \kappa, t)) \quad (8)$$

where $DTW(X, Y)$ is a *Dynamic Time Warp* similarity measure, for the same reasons described in Section IV-C1. Trivially $P_{A^*}(\mathcal{N}, \kappa, t) = P_{ideal}(\mathcal{N}, \kappa, t)$ for all t .

D. Swarm Robustness

We define a swarm's *robustness* along two axes: (1) ability to collectively adapt to temporally varying levels of sensor and actuator noise, and (2) ability to collectively adapt to temporal changes in the swarm size. Both of these axes are well motivated in real world examples, such as underwater environments, mining, and distribution warehouses [15], [21], [26], [46], [58]. In such environments, swarms may have to deal with one or more of: (1) high levels of sensor and actuator noise, (2) adversarial task re-allocation in which robots can leave a sub-swarm working on a certain task at any time, and (3) frequent robot mechanical failures.

1) Sensor and Actuator Noise Robustness:

Intuition: Swarm sensor and actuator noise robustness measures how swarm performance under sensor and actuator noise remains close to performance under ideal, noise-free conditions. We compare performance *curves*, rather than cumulative performance values, in order to account for swarm emergent (partial) mitigation of the applied noise via changing behaviors. In a swarm with optimal sensor and actuator robustness $B_{saa}^*(\mathcal{N}, \kappa)$, $P_{ideal}(\mathcal{N}, \kappa, t) = P(\mathcal{N}, \kappa, t)$.

Definition: $B_{saa}(\mathcal{N}, \kappa)$ is defined as:

$$B_{saa}(\mathcal{N}, \kappa) = CL(P_{ideal}(\mathcal{N}, \kappa, t), P(\mathcal{N}, \kappa, t)) \quad (9)$$

where we define $CL(X, Y)$ to be a *curve length* similarity measure which computes the distance from X_0 to each X_i as a ratio to the total curve length, and then uses this value to compute a pairwise difference with Y_i ; the value of $CL(X, Y)$ is the sum of these differences [45]. This measure was chosen instead of the $DTW(X, Y)$ measure used in Section IV-C because $B_{saa}(\mathcal{N}, \kappa)$ as we have defined it does not consider how slowly or quickly $P(\mathcal{N}, \kappa, t)$ adapts to temporally varying sensor and actuator noise, only how closely it matches $P_{ideal}(\mathcal{N}, \kappa, t)$ in an absolute, time-invariant way.

2) Population Dynamics Robustness:

Since not all robots within \mathcal{S} may be allocated to a task \mathcal{T} of interest at a given point in time, let the sub-swarm $S \subseteq \mathcal{S}$ composed of $N(t)$ robots (which can vary in time) be the portion of \mathcal{S} that is allocated to \mathcal{T} at time t .

Intuition: Swarm *population dynamics robustness* measures the swarm's ability to maintain the same level of performance as population variance increases. That is, as robots enter and leave S over time (permanently or temporarily), they will bring with them inexperience and/or an inaccurate world model as it relates to the task \mathcal{T} that S is working on. Swarms with optimal robustness to population dynamics $B_{pd}^*(\kappa)$ will have the same (or better) performance regardless of the fluctuations of swarm size when compared with ideal conditions for all t .

Derivation: We define three queues to model the possible sources of a temporally varying $N(t)$ [47].

- 1) *Birth queue.* Q_b is a M/M/1/($\mathcal{N} - N(0)$)/0 [49] defined by $(\lambda_b = 0, \mu_b)$, which models the addition of new robots to the swarm that have been released from other tasks to join S to work on its assigned task \mathcal{T} . There are $(\mathcal{N} - N(t))$ places in the queue, corresponding to the number of robots present in \mathcal{S} but that are currently engaged in other tasks at $t = 0$. This queue begins with $(\mathcal{N} - N(0))$ robots in it, and has a finite population.
- 2) *Death queue.* Q_d is a M/M/0/ \mathcal{N} / \mathcal{N} [49] defined by $(\lambda_d, \mu_d = \infty)$ modeling the permanent removal of robots from S as they (1) critically malfunction, or (2) become permanently reallocated to other tasks and are removed from the swarm; the two cases are treated identically in our analysis. There are 0 servers in this queue, and hence $\mu_d = \infty$. It begins with 0 robots in it.
- 3) *Repair/reallocation queue.* Q_r is a M/M/1/ \mathcal{N} / \mathcal{N} (birth-death process) [49] defined by (λ_{bd}, μ_{bd}) modeling the *temporary* removal of robots from S as they (1) non-critically malfunction and are repaired, or (2) become temporarily reallocated to other tasks of relatively short duration, finish those tasks, and return to S to work on \mathcal{T} ; the two cases are treated identically in our analysis. It begins with 0 robots in it.

Assuming that (1) the service/arrival rates are constant, (2) Q_b, Q_d, Q_r are all independent, (3) a robot can be a member of at most one queue at a time, we leverage the additive property of Poisson random variables and combine Q_b, Q_d, Q_r into a single M/M/1/ $N(t)$ / \mathcal{N} queue $Q_{\bar{S}}$ modeling the number of robots *not* in S at t .

To have a stable system, the *utilization* $\rho_{\bar{S}}$ must be < 1 :

$$\rho_{\bar{S}} = \frac{\lambda_d + \lambda_{bd}}{\mu_b + \mu_{bd}} \quad (10)$$

There are multiple ways to achieve the necessary stability within our model, each depending on the relative arrival and service rates of Q_b, Q_d, Q_r . However, the *variance* of the queue size can vary greatly (again depending on the relative arrival and service rates of Q_b, Q_d, Q_r) as robots stay in the swarm for different amounts of time, on average. Using Little's law [49] to calculate the total amount of time each robot spends in $Q_{\bar{S}}$ on average, we have:

$$L_{\bar{S}} = \frac{\rho_{\bar{S}}}{1 - \rho_{\bar{S}}} \quad (11)$$

and the total amount of time $T_{\bar{S}}$ that a robot spends not part of S :

$$T_{\bar{S}} = \frac{1}{\mu_b + \mu_{bd} - (\lambda_d + \lambda_{bd})} - \frac{1}{\mu_b + \mu_{bd}} \quad (12)$$

We can then compute our quantity of interest, the amount of time a robot is *not* in $Q_{\bar{S}}$ (and therefore part of S), by taking $T_S = T - T_{\bar{S}}$.

Higher values of T_S indicate more stable swarms, and lower values indicate more volatile swarms in which more “experienced” robots in the swarm will have to contend with the sub-optimal actions of less experienced (in terms of world model) robots which are newly added, have returned from being repaired, or have finished a different task they were directed to complete.

Definition: $B_{pd}(\kappa)$ is defined as:

$$B_{pd}(\kappa) = \sum_{t \in T} P(N(t), \kappa, t) - \frac{T_S}{T} P_{ideal}(N(t), \kappa, t) \quad (13)$$

and measures the difference between $P_{ideal}(N(t), \kappa, t)$ and $P(N(t), \kappa, t)$, weighted by swarm population variance, $\frac{T_S}{T}$.

V. EXPERIMENTAL FRAMEWORK

The experiments described in this paper have been carried out in the ARGoS simulator [59]. We employ a dynamical physics model of the robots in a three dimensional space for maximum fidelity (robots are still restricted to motion in the XY plane), using a model of the s-bot developed by [60]. For all experiments we average the results of 96 experimental runs of $T = 100,000$ seconds for each κ for the robustness experiments, and $T = 20,000$ seconds for all others.

We utilize the SIERRA (<https://github.com/swarm-robotics/sierra.git>) framework for automatically (1) generating simulation inputs based on a variable of interest (swarm size, level of noise or temporal variance to inject, etc.), (2) running experiments on a variety of computing platforms in parallel, (3) averaging experimental results, (4) generating the graphs seen in this paper. SIERRA utilizes a highly configurable plugin-based architecture, and so was easily adapted and customized to meet the needs of this project.

VI. SCENARIO 1: INDOOR WAREHOUSE

In this scenario, we as SR system designers are tasked with choosing between candidate control algorithms for a system of homogeneous robots which will be deployed to a small ($\sim 500 m^2$) and a medium ($\sim 2000 m^2$) warehouse of an order fulfillment company, which has just expanded from their previous small warehouse, and is looking to upgrade their robotic infrastructure. They previously had 50 robots in their small warehouse, divided into 10 teams of 5 (one team was assigned to assist with filling a given order) and that was enough to meet order demand *most* of the time. The medium warehouse will have the items for online orders spread throughout the floor, and the small warehouse will be repurposed as a distribution relay center in which orders arrive and then go out on one of a set of trucks.

The company has said it is willing to pay for up to 1,000 robots total across both warehouses, but hope that sufficient performance can be achieved with fewer robots. They have done some “back of the napkin” calculations and believe that sufficient throughput can be maintained with $N_{min} = 50$

robots for all algorithms (Section III-B) in their small warehouse, but they have no idea how many robots will be needed in the medium warehouse to keep up with demand. They hope to be able to field a purely robotic workforce on the warehouse floor; however, they are willing to incorporate a few human workers to help manage the floor (e.g., to help with cache maintenance if the STOCHM algorithm is chosen) if the performance benefits are sufficiently large, but would prefer not to in order to avoid potential health hazards.

They do not anticipate further near-term expansion, but given the strong upward trend of their business, they believe they will need to expand into a larger ($\sim 9,000 m^2$) warehouse in the future, and are looking to “future-proof” their robotic infrastructure as much as possible in their algorithm choice.

A. Design Constraints

This scenario, or variants of it with a subset of the design constraints below, has been studied by [8], [24], [26], [32], [56]. Given the company’s description of their scenario, we define the following design constraints:

- $P(\mathcal{N}, \kappa, t)$: Measures the rate of object collection; more efficient control algorithms for \mathcal{S} will gather more objects in a fixed amount of time.
- Operating arena: Fixed size ($500 m^2$, $2,000 m^2$, and $9,000 m^2$) with variable swarm density.
- Object distribution: Random for the medium and large warehouses, and single source for the small warehouse.
- Environmental disturbances: It is a tightly controlled indoor environment unaffected by outside weather patterns, but periodic events such as shift changes, deliveries, and other disturbances may still occur. We model these disturbances as square waves, applying throttling functions to the maximum robot speed while carrying an object, modeling increased congestion and additional computational time needed to plan safe trajectories in the presence of unknown dynamic obstacles while transporting goods. Given that the frequency and disruptiveness of the disturbances is unknown, we test throttling levels $0 - 0.40$, and set the frequency $f = 5000$, modeling periods of intense disruption that appear \sim every 1.4 hours.
- Sensor and actuator noise: It is a tightly controlled indoor environment, and therefore no unexpected sources of sensor or actuator noise will exist; precise indoor localization methods may also be available. However, no SR system is noise free, so we will investigate the effect of minor levels of Gaussian noise $G(\mu, \sigma)$ with $\mu = 0, \sigma = 0 - 0.03$ for better real-world modeling.
- Task reallocations: Given that robots will work alongside humans in all three warehouses, we assume that human employees (or a centralized warehouse AI) will be able to reallocate robots at any time as workloads evolve throughout the day. We do not have an estimate of how often this will occur from the company’s problem description, but given that $N_{min} = 5$, and 50 robots are available we can compute the reallocation rates using Eqs. (1), (10) and (11) for the small warehouse, and extrapolate for the medium and large warehouses as needed.

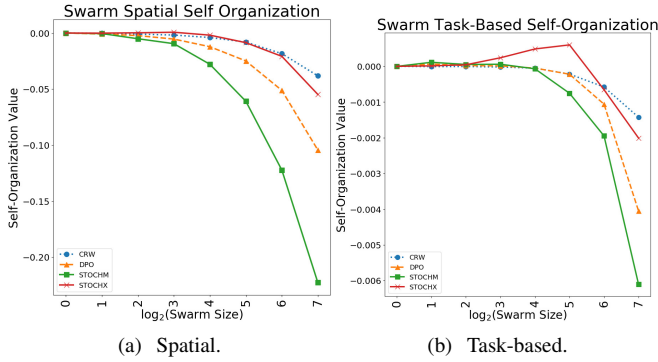


Fig. 5: Swarm emergent self-organization for the small warehouse (32×16 arena) under ideal conditions (no sensor and actuator noise or population dynamics).

- Minimum collective performance: Achieved by $N_{min} = 5$ robots for all candidate control algorithms in the small warehouse, $N_{min} = 5 \times 4 = 20$ in the medium warehouse, extrapolating from the company’s estimate.
- Robot reliability: Given the tightly controlled environment and assumed regular maintenance of robots, the overall robotic temporary failure, repair, permanent failure rates should be extremely low. We set $\lambda_d = 0$ and $\mu_b = 0$, as \mathcal{N} is fixed throughout operation.

We use a $32 \times 16 = 512 m^2$ arena to model the size of the small warehouse, and $\mathcal{N} = 50$, a $48 \times 48 = 2,048 m^2$ arena for the medium warehouse, and a $96 \times 96 = 9,216 m^2$ arena for the large warehouse. We perform a comparative analysis of the robustness, scalability and emergent self-organization, and flexibility of the candidate algorithms described in Section III-B in Sections VI-B to VI-E below.

B. Emergent Self-Organization Analysis

We first examine the emergent self-organization of each κ , as part of recommending an algorithm that is as future-proof as possible given different operating conditions, warehouse layouts, etc.

From Fig. 5 we see moderate levels of CRW spatial self-organization emerge, likely due to sufficiently large perturbations of robot exploratory random walks via interference by robots returning to the nest with objects; this serves as a good benchmark to compare more complex and intuitively “intelligent” algorithms against.

The STOCHX/CRW algorithms have the most consistent level of spatial self-organization across all swarm sizes. This is in good agreement with the *random fluctuations* system property necessary for self-organization to occur, as CRW swarms have the most consistent levels of randomness due to their memory-less nature and random walks, and STOCHX swarms have additional fluctuations due to their stochastic task allocation policies. More striking downward trends are observed with the DPO/STOCHM algorithms, due to the collective learning of the locations of blocks and static caches in the arena, and increased competition for the limited space near them. These phenomena are much more evident at larger swarm sizes, in agreement with our intuition.

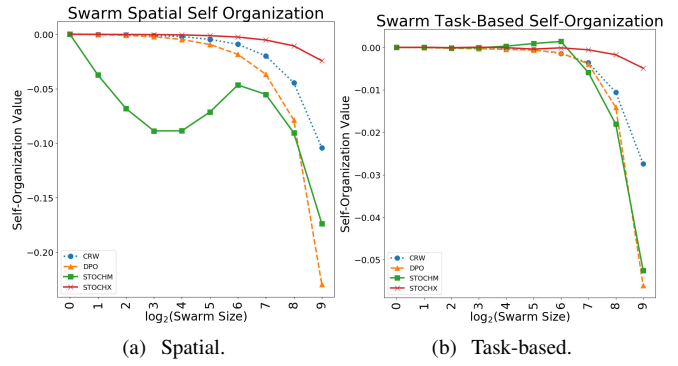


Fig. 6: Swarm emergent self-organization for the medium warehouse (48×48 arena) under ideal conditions (no sensor and actuator noise or population dynamics).

In Fig. 5b, the small arena size restricts the ability of swarms to learn by conflating beneficial inter-robot interactions with excessive collision avoidance. Even the most complex algorithm, the STOCHX algorithm, has lower task-based self-organization than the CRW algorithm at higher swarm sizes due to insufficient swarm density and/or arena size, which leads to less effective of traffic regulation as a result of to dynamic cache creation, utilization, and destruction. The general congruence of the relative ordering of algorithms in both Figs. 5a and 5b suggests that spatial and task-based self-organization are strongly correlated, at least for spatially constrained environments like the one studied here.

Keeping this in mind, we examine the spatial self-organization for all κ (Fig. 6a) in the medium warehouse. The levels of organization achieved are approximately the same as those in the small warehouse (Fig. 5a), because the maximum swarm size (512) is scaled proportionally to the larger arena area ($2,048m^2$). However, we now see clearer separations between all algorithms in terms of their ability to spatially self-organize in spite of this scaling: the larger area reduces the level of inter-robot interactions at swarm sizes ≤ 512 , thus requiring the swarm to collectively learn *more* from fewer interactions, and reducing conflation between different types of inter-robot interactions. As expected, the complex STOCHX algorithm is the most adept at doing this via its dynamic use of caches, especially at larger swarm sizes, in accordance with our intuition.

Similarly, Fig. 6b shows strongly downward trending levels of task-based self organization for all algorithms except STOCHX. Task-based self-organization is a higher level swarm cognitive function, and the STOCHX algorithm is the most complex of all evaluated algorithms, having the greatest intuitive potential for such cognition. Just like the results for the small warehouse, we see a strong congruence in the relative ordering of algorithms in terms of spatial and task-based self-organization levels in Figs. 6a and 6b, providing strong evidence that a quantitative relationship between the two exists. Overall, our results for the medium warehouse are in good agreement with the *multiple interactions* system property necessary for self-organization to occur discussed in Section II,

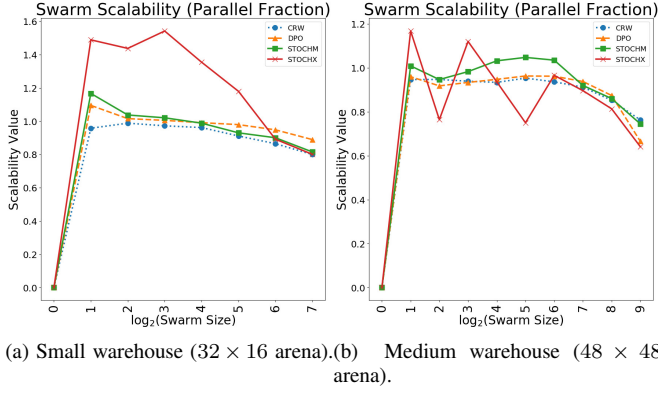


Fig. 7: Swarm scalability under ideal conditions (no sensor and actuator noise or population dynamics).

and with previous work showing that swarm density is the critical factor in developing self-organization [42].

From this, we conclude that the STOCHX algorithm is the most suited from a self-organization standpoint.

C. Scalability Analysis

We next examine the scalability of each κ , as part of recommending an algorithm that is as future-proof as possible, given the company’s plausible future expansion plans into a large warehouse, using variable swarm density within the small and medium warehouses.

From Fig. 7a, we see a strong correlation between self-organization and scalability, with the STOCHX algorithm showing the greatest potential for scalability at smaller swarm sizes in the small warehouse. However, its advantage in scalability via learning *more* from fewer interactions is greatly diminished with increasing swarm sizes in the small space, likely due to the conflation between beneficial and adverse inter-robot interactions mentioned earlier. In Fig. 7b, the STOCHM algorithm generally shows a trend as being the most scalable, as a result of its efficient exploitation of the static caches (in contrast to STOCHX which has to both make *and* exploit dynamic caches).

Extrapolating from our analysis of the small and medium warehouses, we predict that the STOCHM will be most highly performing in a hypothetical future large 96×96 warehouse, which is confirmed by Fig. 8.

We note that even though from the previous section the STOCHX algorithm was the most intelligent, it was the worst performing algorithm in the large warehouse, even lower than CRW (it still meets the minimum collective performance, however, per the scenario specification). Previous work [56] has shown that the STOCHX algorithm outperforms the STOCHM, DPO, and CRW algorithms in dual source foraging (Fig. 2b), an environment much more conducive to the emergence of strong traffic patterns to increase efficiency. The random foraging environment studied here is much more adverse in terms of facilitating such emergence, leading to the observed lower performance. This difference demonstrates the necessity of accurate modeling and thorough analysis

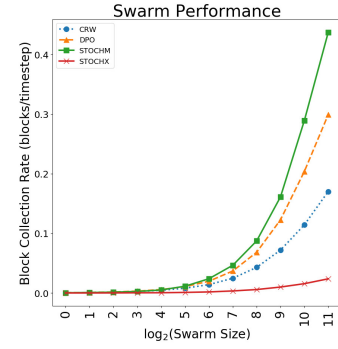
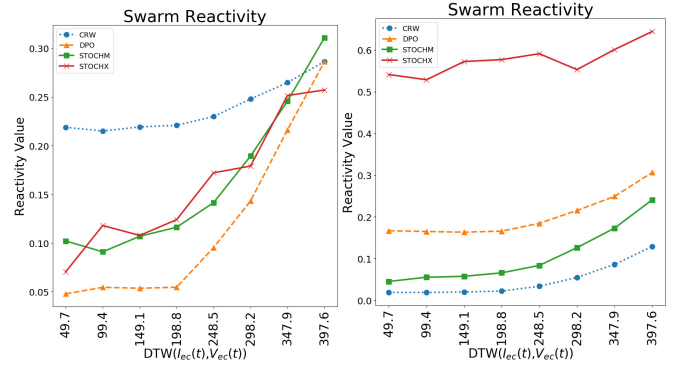


Fig. 8: Raw performance in the large warehouse (96 × 96 arena).



(a) Small warehouse (32 × 16 arena). (b) Medium warehouse (48 × 48 arena).

Fig. 9: Swarm Reactivity $R(\mathcal{N}, \kappa)$ across both warehouses under periodic, high intensity changes in environment adversity (square waves). Distance from ideal environmental conditions is on the X axis, and distance to the ideal reactivity curve $P_{R^*}(\mathcal{N}, \kappa, t)$ is on the Y axis (i.e., lower is better).

when designing SR systems, and the interaction between scenario characteristics and swarm dynamics (e.g., the object distribution model can result in strong orthogonality between scalability and emergent self-organization), and the importance of matching algorithms to environments in which they are naturally well-suited.

From this discussion, we conclude that the STOCHM algorithm is the most scalable. Furthermore, the difference between it and the other algorithms is sufficiently large that the company will likely be willing to invest in human operators in the warehouse in order to maintain the static caching sites needed by the algorithm. Overall, the results of our scalability experiments match very well with our intuitions described in Section III-B.

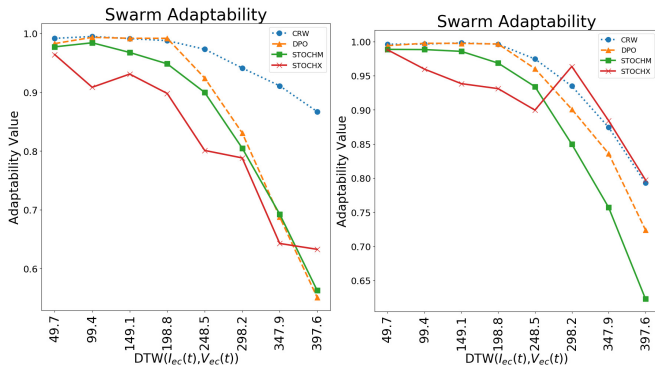
D. Flexibility Analysis

We examine the flexibility of each κ as part of our algorithm recommendation, given potential differences in operating conditions within warehouses due to changing delivery and/or demand schedules throughout the day.

As we can see in Fig. 9, the trendlines are slightly more pronounced for the small warehouse than for the medium one

across all algorithms. This is likely due to the conflation of the experimental variables for inter-robot interference and environmental adversity. In the medium warehouse, because the relative levels of inter-robot interference are lower, we see much more consistent trendlines of approximately the same slope, indicating that all algorithms, regardless of “intelligence”, have nearly identical marginal reactivity to increasingly adverse environmental conditions beyond a unique “setpoint”.

DPO swarms are unable to substantially react to changing environmental conditions because they are fundamentally unable to alter their behavior, which is compounded with increased congestion at shared resources. STOCHM swarms perform better due to their more complex task allocation distributions, confirming our intuition. STOCHX swarms, as expected, are the most reactive of all evaluated algorithms.



(a) Small warehouse (32×16 arena). (b) Medium warehouse (48×48 arena).

Fig. 10: Swarm adaptability $A(\mathcal{N}, \kappa)$ across both warehouses under periodic, high intensity changes in environment adversity (square waves). Distance from ideal environmental conditions is on the X axis, and distance to the ideal adaptability curve $P_{A^*}(\mathcal{N}, \kappa, t)$ is on the Y axis (i.e., lower is better).

We see in Fig. 10 further evidence of synergy between our measures: strong correlation between the relative levels of spatial and task-based self organization for the STOCHM and STOCHX algorithms (Figs. 5 and 6). CRW and STOCHX swarms have the highest levels of self-organization, and the highest reactivity and adaptability as well. However, the DPO and STOCHM algorithms, while more complex than CRW, are not as reactive or adaptive, clearly demonstrating that adding cognitive capacity to a given algorithm is not guaranteed to make the swarm more collectively “intelligent” and flexible.

DPO and STOCHM, as cognitive algorithms (i.e., each robot has memory), will actively try to react and mitigate or exploit environmental conditions as appropriate, while the purely reactive (i.e., memoryless) algorithm CRW did not actively try to do so, which collectively enabled it to be more flexible. However, the even more “intelligent” STOCHX algorithm was more reactive and adaptive than the CRW algorithm for more drastic environmental disturbances, suggesting that it is possible to design a more complex, cognitive algorithm which is just as flexible as a purely reactive algorithm. More work is needed to further explore this relationship, but our results suggest that there is a threshold emergent

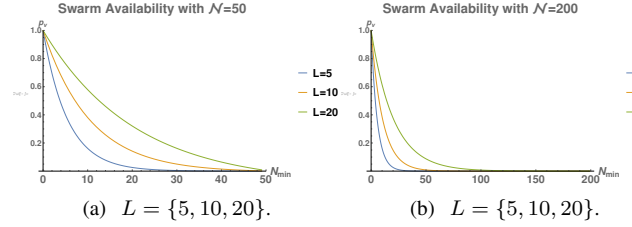
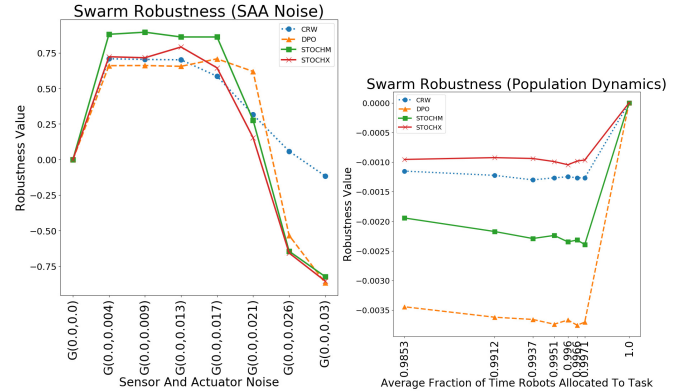


Fig. 11: Available swarm availability p_v for desired steady state swarm sizes $N(t)$ /steady state queue lengths L for different N_{min} .



(a) Swarm sensor and actuator noise (b) Swarm population dynamics robustness ($B_{pd}(\kappa)$).

Fig. 12: Swarm robustness for the small warehouse (32×16 arena size).

self-organization for cognitive algorithms which must be met in order to obtain collective performance which consistently outperforms that of the simpler, biomimetic control algorithms.

From the company’s specification, consistency in performance is more important than exploiting changes in operating conditions. We therefore choose the STOCHX algorithm, which is just as adaptable as the CRW algorithm for small disturbances, which will be likely to be more common in warehouse scenarios than larger ones, and we conclude that it is best suited to their needs from a flexibility standpoint.

E. Robustness Analysis

Finally, we examine swarm robustness in the small and medium warehouses. For the small warehouse, we use $\mathcal{N} = 50$, per the company’s specification, and use Eq. (1) to solve for p_v , given desired steady state $N(t) = \{5, 10, 20\}$, shown in Fig. 11a.

Given that the company thinks they would achieve sufficient performance with $N_{min} = 5$ robots for any algorithm, we see that this corresponds to $p_v \sim 0.40$, meaning that approximately 40% of the time all 5 robots of a given team were available to work on filling a given order. Given that p_v increases substantially if the company reorganizes \mathcal{S} into 5 teams ($p_v \sim 0.65$), we perform our $B_{pd}(\kappa)$ analysis with $\mathcal{N} = 50$, and a target steady state swarm size of $N_{min} = 10$.

For the small warehouse in Fig. 12a, the CRW algorithm is the most robust to sensor and actuator noise, which maps

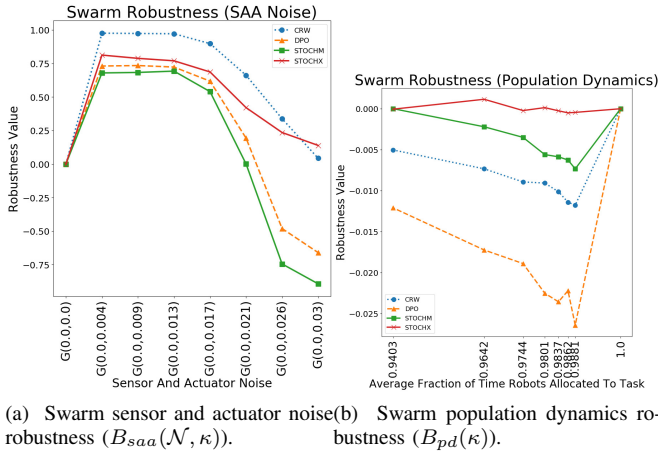


Fig. 13: Swarm robustness for the medium warehouse (48×48 arena size).

well back to our intuition: it is the least reliant on perception and sensors/actuators in general of all evaluated algorithms. All other algorithms rely on sensors and actuators to locate blocks, and therefore have lower robustness at higher noise levels. In Fig. 12b, the self-organization of the STOCHX and CRW algorithms makes them the most robust to fluctuating population sizes, and suggests a loose positive correlation between self-organization and population dynamics robustness, though further work is needed for precise quantification.

For the medium warehouse, we use $\mathcal{N} = 200$, extrapolating from the company’s specification, and use Eq. (1) to solve for p_v , given desired steady state $N(t) = \{5, 10, 20\}$, shown in Fig. 11b.

With $\mathcal{N} = 200$, the availability curves drop off much more steeply, and fielding teams of 10 robots will yield $p_v \sim 0.40$. In order to achieve approximately the same level of availability as the small warehouse, we increase our team size to 20, and perform our $B_{pd}(\kappa)$ analysis with $\mathcal{N} = 200$, and a target steady state swarm size of $N_{min} = 20$.

We see clearer separation between algorithms in the medium warehouse in Fig. 13a, but the same relative ordering as Fig. 12a. In Fig. 13b, we see slightly higher positive levels of population dynamics robustness across all algorithms, given the larger spatial area. The relative ordering between algorithms in the small warehouse seen in Fig. 13b is similar to that in the small warehouse: the STOCHX algorithm is still the most robust to population dynamics, but followed by the STOCHM algorithm rather than the CRW algorithm. This suggests that there are additional factors at play besides self-organization when it comes to population dynamics robustness; one possible explanation is that the large spatial area and cache sizes allowed additional information about the current swarm task distribution to be encoded into the environment, per our intuition.

From the company’s specification, population dynamics robustness is more important than sensor and actuator robustness, hence we conclude that the STOCHX algorithm is best suited to their needs from a robustness standpoint.

We have discussed swarm self-organization, scalability, flex-

ibility, and robustness for the warehouse scenario for all κ and made recommendations for the “best” algorithm for each. It would now be up to the company to take the results of our analysis and determine which of the four main swarm properties were most important to them so they could make a final algorithm decision.

Overall, we see strong evidence in the analyses discussed in this section of the synergistic nature of our derived measures: trends within and between curves on graphs of each can be intuitively explained, and easily mapped back to the technical specifications of a given method in ways that are not evident from raw performance curves alone. This suggests genuine utility and we advocate for their inclusion in the swarm engineer’s toolbox.

VII. SCENARIO 2: OUTDOOR SEARCH AND RESCUE

In this scenario, we as SR system designers are tasked with choosing an appropriate control algorithm for an outdoor search and rescue task for a swarm of homogeneous robots. The system will be deployed in disaster zones/military conflict zones in a fully autonomous fashion as a first response measure, to assess a given outdoor environment and to search for “objects” of interest with the environment. These objects can be unconscious civilians trapped in rubble, places of utility line breaks (e.g., gas lines), which both need to be discovered and reported to human responders or higher level robotic systems as fast as possible in order to minimize loss of life and further infrastructure damage. Not all civilians may be unconscious; some may be conscious and trying to make their way out of the disaster zone or help others, in which case they need to be found and guided to the nearest safe zone. Similarly, the location of utility line breaks may appear to “move” as robot onboard sensing is not powerful enough to provide precise coordinates.

Moderate levels of losses are expected due to the instability of the environment. Therefore, relatively large numbers of robots are desired to ensure mission success. The selected control algorithm needs to be highly scalable and intelligent, so that it can efficiently adapt to a wide range of problem scales and unknown environmental conditions.

A. Design Constraints

This scenario, or variants of it with a subset of the design constraints below, has been studied by [52], [58]. Given the scenario description, we define the following design constraints:

- $P(\mathcal{N}, \kappa, t)$: measures the average minimum time an object remains in the environment before it is picked up for the first time; more efficient control algorithms for \mathcal{S} will learn to discover more objects more quickly.
- Operating arena: Variable size with constant swarm density; size of the area in which targets can be found is not known beforehand. Given the limited sensing capabilities of the robots to be used, and the anticipated robot losses due to malfunction or environmental issues, relatively large swarm sizes should be tested.

- Object distribution: Not known a priori, so random or power law are appropriate models, and we choose power law in this case. Objects can move randomly over time; it is not known how often this happens so we will test with a range of per-timestep random walk probabilities for each target: $\{0, 0.01, 0.026, 0.051\}$.
- Environmental disturbances: Potentially large and quickly (or gradually) evolving environmental disturbances during swarm operation, such that swarm operating conditions can slowly change from favorable to unfavorable (or vice versa), and potentially back again throughout swarm operation (e.g., a passing storm, windy conditions, etc). We apply throttling functions to the maximum robot speed during operation given that the environmental dynamics in our outdoor scenario might vary significantly. We use a sinusoidal disturbance model with throttling amplitudes $0 - 0.4$ and frequency $f = 10000$, modeling cyclically shifting environmental conditions.
- Sensor and actuator noise: Environmental disturbances (e.g., clouds interfering with localization, fluctuating lighting conditions interfering with perception, etc.) may also occur in the arena. It is not known how much noise will result from the disturbances, but they are known to be transitory. Thus, we select a Gaussian noise model $G(\mu, \sigma)$ with $\mu = 0$ as an appropriate model, and test with $\sigma = 0 - 0.1$.
- Robot reliability: Environmental disturbances and the general unpredictability of operating in an outdoor environment may give rise to software and/or hardware artifacts which will cause robots to fail permanently (for the purposes of this time-sensitive task in which ad-hoc field updates are unlikely). We therefore test $\lambda_d = 0 - 0.0007$.
- Task reallocations: No unexpected task reallocations, due to the time sensitivity of the application. We therefore set $\lambda_{bd} = \mu_{bd} = 0$.

In this scenario, there was no mention of target problem sizes, so we cannot do the simple univariate analyses with specific swarm sizes as we did in the first scenario. Instead, we perform *bivariate* analyses between a range of swarm sizes and another variable of interest, and report our results in two dimensional heatmaps. We omit results where possible for clarity.

B. Emergent Self-Organization Analysis

In Fig. 14, we see stronger horizontal trends in emergent spatial self-organization in STOCHM swarms than DPO swarms, indicating that they were less successful in mitigating target movement effects on the swarm’s collective world model regardless of swarm size. Intuitively, the usage of static caches would likely be less useful than (partially) randomized walking. Overall, the DPO algorithm has the highest reported level of spatial self-organization for higher swarm sizes; in comparison to the CRW algorithm (not shown), when the targets move randomly, remembering where they used to be is still helpful because the target is probably still in the vicinity. We also see some vertical trends for both shown algorithms,



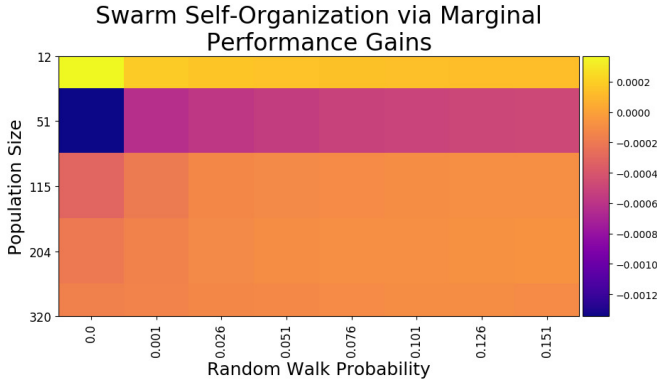
Fig. 14: Swarm emergent spatial self-organization for the search and rescue scenario under ideal conditions (no sensor and actuator noise or population dynamics) for all tested algorithms. The CRW and STOCHX algorithms had much lower levels of emergent spatial self-organization, and were omitted for clarity.

indicating that mitigation of target movement effects was positively correlated with increasing swarm size.

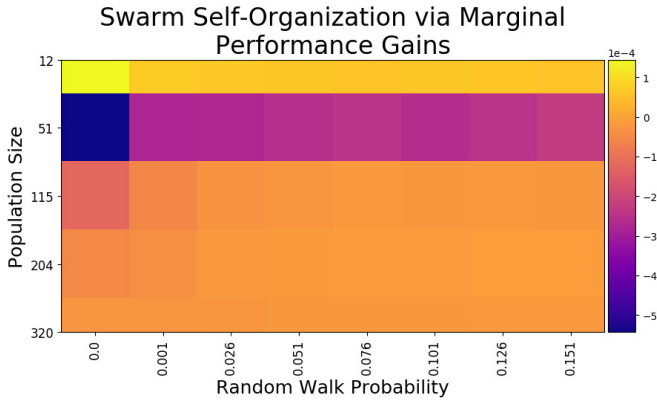
In contrast to the first scenario, in Fig. 15, we see approximately equivalent trends of task-based emergent self-organization for both shown algorithms, with the only difference being the magnitude of the trends. STOCHX exhibited the strongest trends (marginally), and was therefore able to overcome some of the world model errors introduced by target motion through the emergence of specialized task allocation distributions, dynamic cache usage, and bucket brigading which hindered the similar STOCHM algorithm.

From the preceding discussion, we conclude that the DPO algorithm is the best suited to meet the needs of the scenario from a self-organization standpoint, given that (1) efficient usage of limited space is not an issue, (2) dynamic or static caches are of relatively limited utility when targets are in motion, both of which are in agreement with our intuition.

C. Scalability Analysis



(a) DPO algorithm.

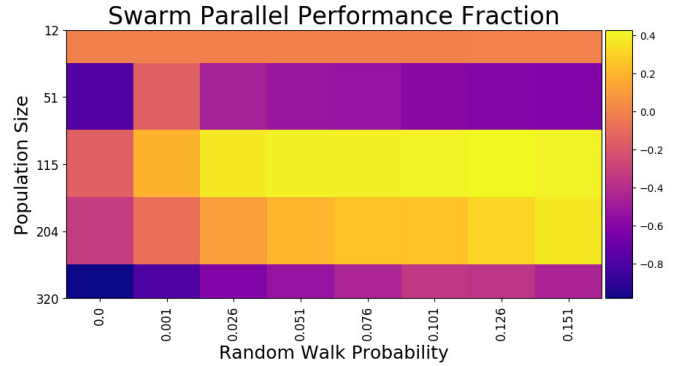


(b) STOCHX algorithm.

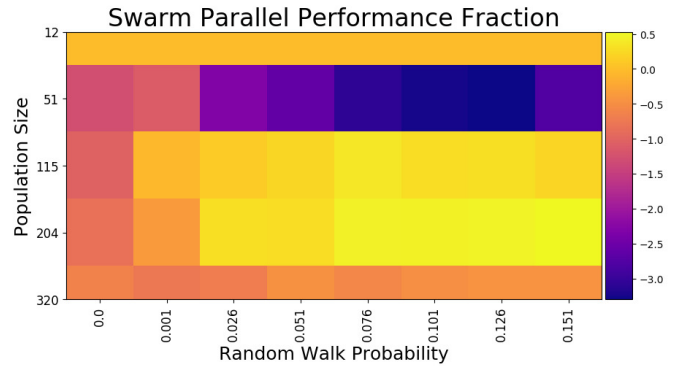
Fig. 15: Swarm emergent task-based self-organization for the search and rescue scenario under ideal conditions (no sensor and actuator noise or population dynamics) for all tested algorithms. The CRW and STOCHX algorithms had much lower levels of emergent task-based self-organization.

From Fig. 16, we see much stronger horizontal than vertical trends across all shown algorithms, indicating that reactivity was more strongly affected by target movement rates than swarm size (as we would expect for constant density experiments). The STOCHX algorithm was the most scalable, being less sensitive to target movement rates than DPO, and achieving peak scalability values at higher swarm sizes, and is therefore best suited to the scalability needs of this scenario.

We note here that in contrast to the dual source Fig. 2b model studied by [56], the power law target distribution studied here is not nearly as conducive to self-organization, which results in the lower scalability values across all algorithms seen here. In addition, constant density swarms further lower the self-organization potential of the environment, resulting in lower scalability and self-organization values than the first scenario. Our findings on this and the previous scenario are in rough agreement with the positive correlation hypothesis between self-organization and performance/scalability from [56]: algorithms with higher levels of self-organization perform better and are more scalable. However, our results in the two studied scenarios suggest that raw comparison of self-organization curves is not sufficient, because different algo-



(a) DPO algorithm.



(b) STOCHX algorithm.

Fig. 16: Swarm scalability for the search and rescue scenario under ideal conditions (no sensor and actuator noise or population dynamics) for all tested algorithms. The CRW and STOCHM were found to be much less scalable, and their results were omitted for clarity.

gorithms require different levels of self-organization to achieve the same performance.

Finally, due to the lack of strong evidence for the effect of target movement rates on swarm scalability and emergent self-organization, we set a constant moderate target movement rate of 0.001 to simplify the rest of our analyses.

D. Flexibility Analysis

In Fig. 17, the swarm size corresponding to maximum reactivity is higher for DPO swarms. This is likely to be due to the relatively constant level of inter-robot interactions requiring the swarm to learn *more* from each interaction, which is more evident at larger swarm sizes. Much of the learning of STOCHM swarms to utilize caches is wasted due to the unconstrained nature of the environment and target motion, confirming our intuition from Section III-B regarding DPO vs STOCHM reactivity.

In Fig. 18, we have omitted the results for the CRW and STOCHX algorithms for clarity, as they had similar trends to the STOCHM and DPO algorithms, and much lower values. We see a lack of strong trends for the STOCHM and DPO algorithms, other than general increasing adaptability as the environment becomes more adverse.

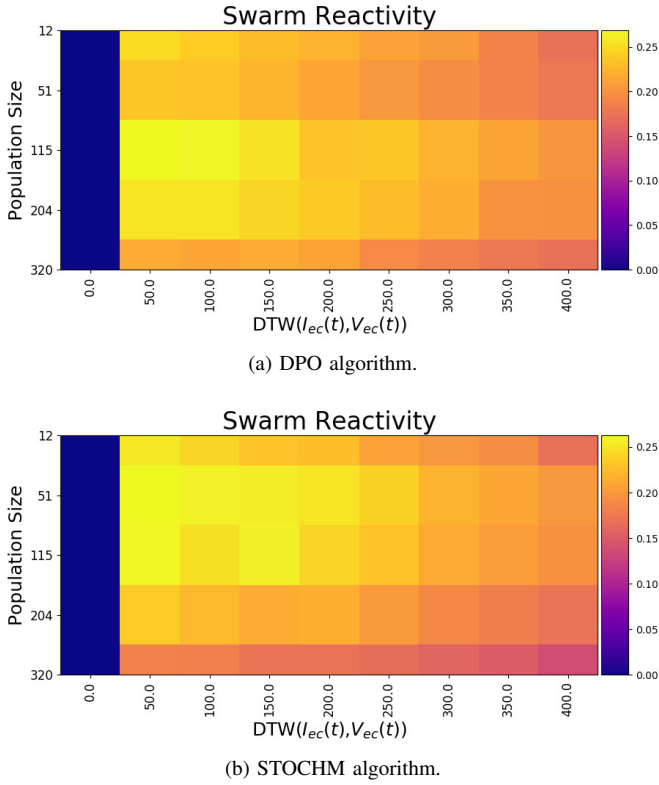


Fig. 17: Swarm reactivity for the search and rescue scenario with constant swarm density under periodic fluctuations in environmental adversity. Distance from ideal environmental conditions on the X axis, swarm size on the Y axis, and distance to the ideal reactivity curve $P_{R^*}(\mathcal{N}, \kappa, t)$ on the Z axis. The CRW and STOCHX algorithms had much lower reactivity and similar trends, and were omitted for clarity.

No matter how “intelligent” a control algorithm may be, there is always an upper limit to its ability to react and/or adapt to environmental conditions, and the conditions tested here appear to show that threshold for the DPO and STOCHM algorithms. There is a split point above which the swarms begin to show increasing levels of adaptability (~ 200 for DPO swarms, ~ 250 for STOCHM swarms), indicating that DPO swarms are *more* adaptable than STOCHM swarms, likely due to the lack of restrictions placed on robot motion due to caches.

From the preceding discussion, we conclude that the DPO algorithm is the most flexible, due to its lack of cache usage, which has been shown to be of limited utility in unconstrained operating environments with constant swarm density.

E. Robustness Analysis

For sensor and actuator noise robustness, we omit the graphs of the results for all algorithms because CRW was the only algorithm which had any measurable levels of robustness to the high levels of noise present in this scenario. Its random search strategy and low reliance on the accuracy of sensor and actuators during operation are likely the main factors

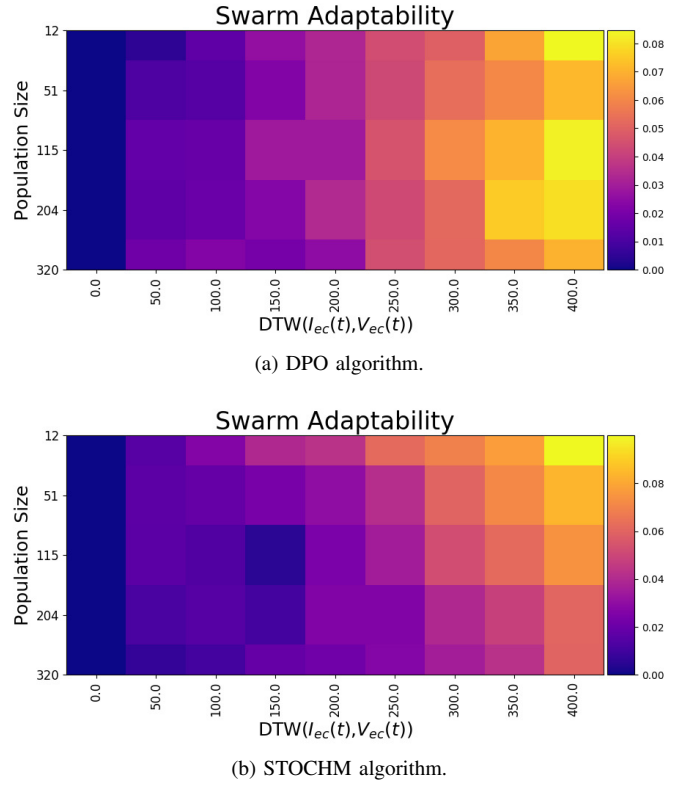


Fig. 18: Swarm adaptability for the search and rescue scenario with constant swarm density under periodic fluctuations in environmental adversity. Distance from ideal environmental conditions on the X axis, swarm size on the Y axis, and distance to the ideal reactivity curve $P_{A^*}(\mathcal{N}, \kappa, t)$ on the Z axis. The CRW and STOCHX algorithms had much lower adaptability, and were omitted for clarity.

behind this. This directly corresponds to our intuition: the more reliant a swarm control algorithm is on accurate sensor and actuator information, the less robust it is going to be to adverse environmental conditions which negatively affect sensors and actuators. In Fig. 19, we focus our analysis on the DPO and STOCHX algorithms. We see similar levels and maximum values of population dynamics robustness for the STOCHM and the DPO algorithms; however the trends of the STOCHM algorithm are generally stronger in the heatmap, indicating greater robustness overall. The large spatial area and cache sizes likely allowed additional information about the current swarm task distribution to be encoded into the environment, resulting in higher robustness, per our intuition. From the preceding discussion, we conclude that the DPO algorithm is the most robust.

In this scenario, we have again seen quantitative confirmation of our intuitions for each κ through our derived measurements for each of the swarm properties of self-organization, scalability, flexibility, and robustness, and made algorithm recommendations. It would now be up to project managers/company/etc., to take our recommendations and make a final decision. However, our results suggest that the DPO algorithm is, on the whole, best suited to the outdoor search and rescue application.

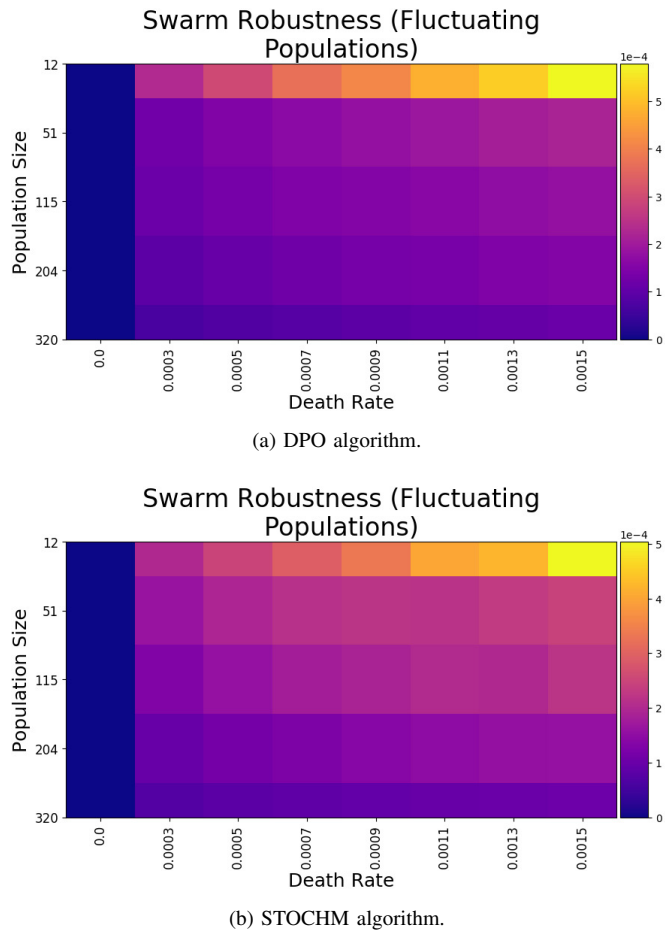


Fig. 19: Swarm population dynamics robustness for the search and rescue scenario with constant swarm density. The CRW and STOCHX algorithms had much lower population dynamics robustness, and were omitted for clarity.

VIII. DISCUSSION

The application of our proposed measures in Sections VI and VII provides a weakly inductive proof of their correctness and utility within the foraging domain, if not more broadly. Despite fundamental differences in characteristics between this scenario and the indoor warehouse, our measurements nevertheless were able to expose the same underlying traits of each controller. Our proposed measures have been shown to provide crucial insights into algorithm design, comparison, and selection for SR systems not easily obtainable from simply comparing raw performance results. They are insightful tools for making theoretically grounded algorithm selection decisions from high level algorithm descriptions (such as those we presented in Section III) for many real-world applications beyond the foraging tasks discussed here, and we argue for their inclusion in the SR system design process as a valuable tool in the swarm engineer’s toolbox.

IX. CONCLUSIONS AND FUTURE WORK

We have presented a measurement methodology for more precise characterization of swarm scalability, emergence, flexibility, and robustness in order to provide mathematical tools to

aid in the iterative design process of SR systems within swarm engineering. We demonstrated the utility of our methodology in the context of two different foraging tasks under various design constraints, and have shown that they provide intuitive insight into recommending a given method for a wide spectrum of problem domains. Next steps in this research would include (1) developing a method for correlating the presented measures with the convergence of the collective swarm solution search, (2) applying our methodology to other domains within SR, such as collective transport, pattern formation, etc, and (3) investigating the orthogonality discovered between some of the axes within our derived measures. In order to facilitate future research and collaboration, the code used for this research is open source, and can be found at <https://github.com/swarm-robotics/fordyca>.

ACKNOWLEDGEMENTS

We gratefully acknowledge Amazon Robotics, the Mn-DRIVE RSAM initiative at the University of Minnesota, and the Minnesota Supercomputing Institute for their support, and London Lowmanstone for his help in the initial experimental framework.

REFERENCES

- [1] E. Şahin, “Swarm robotics: From sources of inspiration to domains of application,” in *Swarm Robotics*, ser. LNCS 3342. Springer, 2005, pp. 10–20.
- [2] T. H. Labella and M. Dorigo, “Division of labor in a group of robots inspired by ants’ foraging behavior,” *ACM Trans. on Autonomous and Adaptive Systems (TAAS)*, vol. 1, no. 1, pp. 4–25, Sep. 2006.
- [3] K. Lerman, A. Martinoli, and A. Galstyan, “A review of probabilistic macroscopic models for swarm robotic systems,” in *Swarm Robotics. SR 2004*, E. Şahin and W. Spears, Eds. Springer Berlin Heidelberg, 2004, vol. LNCS 3342.
- [4] M. Cotsaftis, “An emergence principle for complex systems,” in *Complex Sciences*. Springer Berlin Heidelberg, 2009, pp. 1105–1117.
- [5] A. F. T. Winfield and J. Sa, “On formal specification of emergent behaviours in swarm robotic systems,” *Science*, pp. 363–371, 2005.
- [6] A. Galstyan, T. Hogg, and K. Lerman, “Modeling and mathematical analysis of swarms of microscopic robots,” in *Proc. IEEE Swarm Intelligence Symposium, SIS 2005*, 2005, pp. 209–216.
- [7] C. Szabo, Y. M. Teo, and G. K. Chengleput, “Understanding complex systems: Using interaction as a measure of emergence,” in *Proc. Winter Simulation Conference*, Dec 2014, pp. 207–218.
- [8] J. Harwell and M. Gini, “Broadening applicability of swarm-robotic foraging through constraint relaxation,” *IEEE Int’l Conf. on Simulation, Modeling, and Programming for Autonomous Robots (SIMPAN)*, pp. 116–122, 2018.
- [9] A. F. T. Winfield, W. Liu, J. Nembrini, and A. Martinoli, “Modelling a wireless connected swarm of mobile robots,” *Swarm Intelligence*, vol. 2, no. 2-4, pp. 241–266, Dec. 2008.
- [10] M. Brambilla, E. Ferrante, M. Birattari, and M. Dorigo, “Swarm robotics: A review from the swarm engineering perspective,” *Swarm Intelligence*, vol. 7, no. 1, pp. 1–41, 2013.
- [11] A. F. T. Winfield, C. J. Harper, and J. Nembrini, “Towards dependable swarms and a new discipline of swarm engineering,” in *Swarm Robotics. SR 2004. Lecture Notes in Computer Science*. Springer, 2005, vol. LNCS 3342, pp. 126–142.
- [12] J. P. Hecker and M. E. Moses, “Beyond pheromones: evolving error-tolerant, flexible, and scalable ant-inspired robot swarms,” *Swarm Intelligence*, vol. 9, no. 1, pp. 43–70, 2015.
- [13] J. Harwell and M. Gini, “Swarm engineering through quantitative measurement of swarm robotic principles in a 10,000 robot swarm,” *International Joint Conference on Artificial Intelligence (IJCAI)*, 2019.
- [14] S. Berman, Á. Halász, V. Kumar, and S. Pratt, “Algorithms for the analysis and synthesis of a bio-inspired swarm robotic system,” in *Swarm Robotics*. Springer-Verlag Berlin Heidelberg, 2007, vol. LNCS 4433, pp. 56–70.

- [15] K. Lerman, A. Galstyan, T. Hogg, and H.-P. Labs, "Mathematical analysis of multi-agent systems," arXiv:cs/0404002 [cs.RO], pp. 1–42, 2004.
- [16] C. Dixon, A. Winfield, and M. Fisher, "Towards temporal verification of emergent behaviours in swarm robotic systems," in *Lecture Notes in Computer Science*, 2011, vol. LNAI 6856, pp. 336–347.
- [17] A. Campo and M. Dorigo, "Efficient multi-foraging in swarm robotics," in *Advances in Artificial Life, LNAI 4648*. Springer, 2007.
- [18] A. E. Turgut, H. Çelikkanat, F. Gökçe, and E. Şahin, "Self-organized flocking in mobile robot swarms," *Swarm Intelligence*, vol. 2, no. 2-4, pp. 97–120, 2008.
- [19] N. Correll, "Parameter estimation and optimal control of swarm-robotic systems: A case study in distributed task allocation," in *Proc. IEEE Int'l Conf. on Robotics and Automation*, May 2008, pp. 3302–3307.
- [20] M. Dorigo, V. Trianni, E. Şahin, R. Groß, T. H. Labella, G. Baldassarre, S. Nolfi, J. L. Deneubourg, F. Mondada, D. Floreano, and L. M. Gambardella, "Evolving self-organizing behaviors for a swarm-bot," *Autonomous Robots*, vol. 17, no. 2-3, pp. 223–245, 2004.
- [21] M. Duarte, V. Costa, J. Gomes, T. Rodrigues, F. Silva, S. M. Oliveira, and A. L. Christensen, "Evolution of collective behaviors for a real swarm of aquatic surface robots," *PLoS ONE*, vol. 11, no. 3, pp. 1–25, 2016.
- [22] E. Ferrante, A. E. Turgut, E. Duéñez-Guzmán, M. Dorigo, and T. Wenseleers, "Evolution of Self-Organized Task Specialization in Robot Swarms," *PLoS Computational Biology*, vol. 11, no. 8, 2015.
- [23] K. Lerman, A. Galstyan, A. Martinoli, and A. Ijspeert, "A macroscopic analytical model of collaboration in distributed robotic systems," *Artificial Life*, vol. 7, no. 4, pp. 375–393, 2001.
- [24] E. Castello, T. Yamamoto, F. D. Libera, W. Liu, A. F. Winfield, Y. Nakamura, and H. Ishiguro, "Adaptive foraging for simulated and real robotic swarms: the dynamical response threshold approach," *Swarm Intelligence*, vol. 10, no. 1, pp. 1–31, 2016.
- [25] E. Ferrante, E. Duenez-Guzman, A. E. Turgut, and T. Wenseleers, "GESwarm: grammatical evolution for the automatic synthesis of collective behaviors in swarm robotics," *Proc. Conf. on Genetic and Evolutionary Computation (GECCO)*, pp. 17–24, 2013.
- [26] G. Pini, A. Brutschy, M. Frison, A. Roli, M. Dorigo, and M. Birattari, "Task partitioning in swarms of robots: An adaptive method for strategy selection," *Swarm Intelligence*, vol. 5, no. 3-4, pp. 283–304, 2011.
- [27] L. Matthey, S. Berman, and V. Kumar, "Stochastic strategies for a swarm robotic assembly system," *Proc. IEEE Int'l Conf. on Robotics and Automation*, pp. 1953–1958, 2009.
- [28] Y. K. Lopes, S. M. Trenkwalder, A. B. Leal, T. J. Dodd, and R. Groß, "Supervisory control theory applied to swarm robotics," *Swarm Intelligence*, vol. 10, no. 1, pp. 65–97, 2016.
- [29] H. Hamann, "Towards swarm calculus: urn models of collective decisions and universal properties of swarm performance," *Swarm Intelligence*, vol. 7, pp. 145–172, 2013.
- [30] H. Hamann and H. Wörn, "A framework of space-time continuous models for algorithm design in swarm robotics," *Swarm Intelligence*, vol. 2, no. 2-4, pp. 209–239, 2008.
- [31] B. Liu, T. Chu, and L. Wang, "Collective motion in non-reciprocal swarms," *Journal of Control Theory and Applications*, vol. 7, no. 2, pp. 105–111, 2009.
- [32] G. Pini, A. Brutschy, M. Birattari, and M. Dorigo, "Task partitioning in swarms of robots: Reducing performance losses due to interference at shared resources," in *Informatics in Control Automation and Robotics*, ser. LNEE 85. Springer, 2011, pp. 217–228.
- [33] A. H. Karp and H. P. Flatt, "Measuring parallel processor performance," *Commun. ACM*, vol. 33, no. 5, pp. 539–543, May 1990.
- [34] E. Bonabeau, M. Dorigo, D. d. R. D. F. Marco, G. Theraulaz, G. Theraulaz et al., *Swarm intelligence: from natural to artificial systems*. Oxford University Press, 1999, no. 1.
- [35] N. Correll and A. Martinoli, *Towards optimal control of self-organized robotic inspection systems*. IFAC, 2006, vol. 8, no. PART 1.
- [36] D. Payton, M. Daily, R. Estowski, M. Howard, and C. Lee, "Pheromone robotics," *Autonomous Robots*, vol. 11, no. 3, pp. 319–324, 2001.
- [37] J.-P. Georgé and M.-P. Gleizes, "Experiments in Emergent Programming Using Self-organizing Multi-agent Systems," *Multi-Agent Systems and Applications IV*, vol. 3690, pp. 450–459, 2005.
- [38] H. Li, T. Wang, H. Wei, and C. Meng, "Response strategy to environmental cues for modular robots with self-assembly from swarm to articulated robots," *Journal of Intelligent and Robotic Systems: Theory and Applications*, vol. 81, no. 3-4, pp. 359–376, 2016.
- [39] W. Liu, a. F. T. Winfield, J. Sa, J. Chen, and L. Dou, "Towards energy optimization: Emergent task allocation in a swarm of foraging robots," *Adaptive Behavior*, vol. 15, no. 3, pp. 289–305, 2007.
- [40] M. Frison, N. L. Tran, N. Baiboun, A. Brutschy, G. Pini, A. Roli, M. Dorigo, and M. Birattari, "Self-organized task partitioning in a swarm of robots," in *Swarm Intelligence*. Springer, Berlin, Heidelberg, 2010, vol. LNCS 6234, pp. 287–298.
- [41] K. Sugawara, I. Yoshihara, K. Abe, and M. Sano, "Cooperative behavior of interacting robots," *Artificial Life and Robotics*, vol. 2, no. 2, pp. 62–67, 1998.
- [42] K. Sugawara and M. Sano, "Cooperative acceleration of task performance: Foraging behavior of interacting multi-robots system," *Physica D: Nonlinear Phenomena*, vol. 100, no. 3-4, pp. 343–354, 1997.
- [43] G. Beni and J. Wang, "Swarm intelligence in cellular robotic systems," in *Robots and Biological Systems: Towards a New Bionics?*, P. Dario, G. Sandini, and P. Aebischer, Eds. Berlin, Heidelberg: Springer Berlin Heidelberg, 1993, pp. 703–712.
- [44] A. Rosenfeld, G. A. Kaminka, and S. Kraus, "A study of scalability properties in robotic teams," in *Coordination of Large-Scale Multiagent Systems*, 2006, pp. 27–51.
- [45] C. F. Jekel, G. Venter, M. P. Venter, N. Stander, and R. T. Haftka, "Similarity measures for identifying material parameters from hysteresis loops using inverse analysis," *International Journal of Material Forming*, pp. 1–24, 2018.
- [46] T. W. Hsieh, M. Ani, Mather, "Robustness in the Presence of Task Differentiation in Robot Ensembles," *Redundancy in Robot Manipulators and Multi-Robot Systems*, pp. 93–108, 2013.
- [47] Y. Zhang, F. Bastani, I. L. Yen, F. Jheng, and I. R. Chen, "Availability analysis of robotic swarm systems," *Proc. 14th IEEE Pacific Rim Int'l Symposium on Dependable Computing, PRDC 2008*, pp. 331–338, 2008.
- [48] R. Zhang and M. Pavone, "Control of robotic mobility-on-demand systems: A queueing-theoretical perspective," *The International Journal of Robotics Research*, vol. 35, no. 3, pp. 186–203, 2016.
- [49] M. Šeda, J. Šedová, and M. Horký, "Models and simulations of queueing systems," in *Recent Advances in Soft Computing. ICSC-MENDEL 2016. Advances in Intelligent Systems and Computing, vol 576*, R. Matoušek, Ed., 2017.
- [50] K. Lerman and A. Galstyan, "Agent memory and adaptation in multi-agent systems," *Proc. Int'l Conference on Autonomous Agents*, vol. 2, pp. 797–803, 2003.
- [51] K. Lerman, C. Jones, A. Galstyan, and M. J. Mataric, "Analysis of dynamic task allocation in multi-robot systems," *International Journal of Robotics Research*, vol. 25, no. 3, pp. 225–241, 2006.
- [52] V. Kumar and F. Sahin, "Cognitive maps in swarm robots for the mine detection application," *Proc. IEEE Int'l Conference on Systems, Man and Cybernetics*, vol. 4, pp. 3364–3369, 2003.
- [53] C. Rouff et al., "Properties of a formal method for prediction of emergent behaviors in swarm-based systems," in *Proc. 2nd International Conference on Software Engineering and Formal Methods*, 2004.
- [54] J. Werfel, K. Petersen, and R. Nagpal, "Distributed multi-robot algorithms for the TERMES 3D collective construction system," in *Proc. IEEE/RSJ Int. Conf. on Intelligent Robots and Systems*, 2011, pp. 1–6.
- [55] C. Rouff, "Intelligence in future NASA swarm-based missions," in *Regarding the Intelligence in Distributed Intelligent Systems, Papers from the 2007 AAAI Fall Symposium*, T. Finin, L. Kagal, E. F. Kendall, J. H. Li, M. Lyell, and W. Truszkowski, Eds., 2007, vol. AAAI, FS-07-06, pp. 112–115.
- [56] J. Harwell, L. Lowmanstone, and M. Gini, "Demystifying emergent intelligence and its effect on performance in large robot swarms," *Autonomous Agents and Multi-Agent Systems (AAMAS)*, 2020.
- [57] V. Gazi and K. M. Passino, "Stability Analysis of Social Foraging Swarms," *IEEE Transactions on Systems, Man, and Cybernetics, Part B: Cybernetics*, vol. 34, no. 1, pp. 539–557, 2004.
- [58] M. A. Hsieh, Á. Halász, S. Berman, and V. Kumar, "Biologically inspired redistribution of a swarm of robots among multiple sites," *Swarm Intelligence*, vol. 2, no. 2-4, pp. 121–141, 2008.
- [59] C. Pinciroli et al., "ARGoS: a modular, parallel, multi-engine simulator for multi-robot systems," *Swarm Intelligence*, vol. 6, no. 4, pp. 271–295, 2012.
- [60] M. Dorigo, "Swarm-bot: An experiment in swarm robotics," in *Proc. IEEE Swarm Intelligence Symposium*, 2005, pp. 199–207.